

**FORT NELSON CCS PROJECT
RESERVOIR QUALITY ASSESSMENT AND
ACID GAS INJECTION STUDY
LABORATORY EVALUATION**

Prepared for:

Energy & Environmental Research Center



Prepared by:

RPS ENERGY

AUGUST 2011

August 9, 2011

Job No. CC00363

Energy and Environmental Research Center
15 North 23rd Street, Sop 9018
Grand Forks, ND 58202-9018

Attention: Mr. Steven Smith
Research Manager

**Re: FORT NELSON CCS PROJECT RESERVOIR QUALITY ASSESSMENT AND ACID GAS INJECTION
STUDY LABORATORY EVALUATION**

Dear Sir:

Please find attached our final report documenting the results of the series of laboratory core tests and the reservoir quality assessment of the Ft. Simpson, Muskwa, Otter Park, Lower Slave Point and Lower Keg River formations of the SECCS Milo c-61-E/94-J-10 well.

The measured cap rock properties, including the mercury injection capillary pressures, the cap rock integrity tests and the mechanical properties tests all indicate that the shale cap rock sequences within the Milo area should remain highly competent even when exposed to acid gas. The rock compressive strengths and threshold intrusion pressures for the subject Ft. Simpson, Muskwa and Otter Park shales are well above the anticipated acid gas storage scheme operating parameters currently envisioned for the Fort Nelson Milo CCS project. The absolute effective permeabilities after exposure to acid gas remain much less than the 0.001 mD value, the highest acceptable cap rock permeability typically recognised for acid gas sequestration schemes.

We appreciate the opportunity to conduct this evaluation for the EERC and should you have any questions or comments on our report, please do not hesitate to contact us.

Yours sincerely,

RPS Energy



Debra Carle
Reservoir and Well Test Specialist
Encl.

TABLE OF CONTENTS

	Page
LETTER OF TRANSMITTAL	
1.0 EXECUTIVE SUMMARY	1-1
1.1 Laboratory Test Objectives within Context of Spectra Energy's CCS Project	1-1
1.2 Conclusions and Recommendations	1-1
2.0 INTRODUCTION	2-1
2.1 Carbon Capture and Storage (CCS)	2-1
2.2 PCOR Partnership and Spectra Energy	2-1
2.3 Fort Nelson CCS Project Area	2-1
2.4 Properties of Cap Rock	2-2
2.5 Properties of Milo Acid Gas	2-3
2.6 Composition of Milo Equilibrium Brine	2-5
2.7 Core Sample Selection and Preparation	2-6
3.0 MERCURY INJECTION CAPILLARY TESTING	3-1
4.0 ROCK MECHANICS	4-1
4.1 Mechanical Testing	4-1
4.2 Cap Rock Integrity Testing	4-6
5.0 RELATIVE PERMEABILITY TESTING	5-1
6.0 CO₂ AND H₂S SOLUBILITY TESTING	6-1
6.1 Bulk Solubility Testing	6-1
6.2 Preferential Solubility Testing	6-1
7.0 REFERENCES	7-1

TABLE OF CONTENTS

LIST OF TABLES

Table 2-1: Composition of Synthetic Formation Brine.....	2-5
Table 2-2: Summary of All Milo c-61-E Core Test Sample Depths	2-7
Table 2-3: Summary of Routine Core Parameters.....	2-9
Table 3-1: Pore Size Distribution and TIP Values.....	3-1
Table 4-1: Summary of Static and Dynamic Elastic Constants	4-3
Table 4-2: Cap Rock Integrity Test Results for Ft. Simpson Shale	4-9
Table 4-3: Cap Rock Integrity Test Results for Muskwa Shale	4-10
Table 4-4: Summary of Shale Cap Rock Integrity Results	4-10
Table 5-1: Summary of Acid Gas/Equilibrium Brine Relative Permeability Results - Primary Drainage	5-3
Table 5-2: Summary of Acid Gas/Equilibrium Brine Relative Permeability Results - Secondary Imbibition	5-4
Table 6-1: Results of Preferential Solubility Test	6-2

LIST OF FIGURES

Figure 2-1: PVT Behaviour of CO ₂	2-4
Figure 2-2: Milo Acid Gas (CO ₂ 95%, H ₂ S 4.4%, N ₂ 0.11%, C1 0.49%) Pressure vs Temperature	2-4
Figure 2-3: Milo Acid Gas (CO ₂ 95%, H ₂ S 4.4%, N ₂ 0.11%, C1 0.49%) Pressure vs Density.....	2-5
Figure 2-4: Schematic Diagram of All Milo c-61-E Core Samples and DST Intervals	2-8
Figure 3-1: Milo c-61-E Samples Pore Size Distribution.....	3-2
Figure 3-2: Threshold Injection Pressure versus Median Pore Size	3-3
Figure 4-1: CT Scan of Muskwa Core Intervals.....	4-1
Figure 4-2: Single Stage Triaxial Compressive Strength Test on Sample MP1	4-4
Figure 4-3: Multi-Stage Triaxial Compressive Strength Test on Sample MP2	4-5
Figure 4-4: Mohr-Coulumb Failure Analysis Results	4-6
Figure 4-5: CT Scan for Ft. Simpson Shale Core Sample (2031.0 m)	4-7
Figure 4-6: CT Scan for Muskwa Shale Core Sample (2048.0 m)	4-8
Figure 5-1: Unsteady State Relative Permeability Test Schematic.....	5-3
Figure 5-2: Acid Gas/Equilibrium Brine Relative Permeability Test Results - Primary Drainage	5-5
Figure 5-3: Acid Gas/Equilibrium Brine Relative Permeability Test Results - Secondary Imbibition	5-5
Figure 5-4: Comparison of Lower Slave Point Drainage Curves with “Low” k and Shale Zones	5-6
Figure 5-5: Comparison of Lower Slave Point Imbibition Curves with “Low” k and Shale Zones	5-6

TABLE OF CONTENTS

LIST OF APPENDICES

- Appendix 1 Detailed Description of Coring Attempts at the SECCS Milo c-61-E/94-J-10 Well
- Appendix 2 Photos of Sampling Attempts in the Shale Zones
- Appendix 3 Labeled Photos of All Core Samples Selected for Testing
- Appendix 4 Understanding the Elastic Parameters

LEGAL NOTICE

This document was prepared by RPS Energy Canada Ltd. (operating as RPS Energy) solely for the benefit of the Energy and Environmental Research Center.

Neither RPS Energy, their parent corporations or affiliates, nor any person acting in their behalf:

- makes any warranty, expressed or implied, with respect to the use of any information or methods disclosed in this document; or
- assumes any liability with respect to the use of any information or methods disclosed in this document.

Any recipient of this document, by their acceptance or use of this document, releases RPS Energy and their sub-contractors, their parent corporations and affiliates from any liability for direct, indirect, consequential, or special loss or damage whether arising in contract, warranty, express or implied, tort or otherwise, and irrespective of fault, negligence, and strict liability.

Project Title	FORT NELSON CCS PROJECT RESERVOIR QUALITY ASSESSMENT AND ACID GAS INJECTION STUDY LABORATORY EVALUATION		
Project Number	CC00363		
		Date of Issue	August 2011
	AUTHOR:	Project Manager	Peer Review
Name	Debra Carle	Lyle Burke	Lyle Burke
File Location:	RPS Energy Canada Suite 1400, 800 – 5th Avenue SW Calgary, Alberta T2P 3T6 T: (403) 265-7226 F : (403) 269-3175 E : rpscal@rpsgroup.com		

1.0 EXECUTIVE SUMMARY

1.1 Laboratory Test Objectives within Context of Spectra Energy's CCS Project

Spectra Energy is currently assessing the feasibility of developing a world-scale integrated carbon capture and storage (CCS) project for the Fort Nelson natural gas plant in northeast British Columbia. This project has been designated as a PCOR project and EERC requested that RPS provide technical support to manage various laboratory activities conducted by Weatherford Laboratories that were designed to assist with the planning of this large-scale CCS project.

The original intent of the extensive coring program for the SECCS MILO c-61-E / 94-J-10 well in the Milo area, NE BC, was to recover sufficient core for detailed analyses from the main reservoir rocks that have been identified as potential injection candidates (Sulphur Point, Keg River and possibly the Slave Point). However, although numerous attempts were made to cut core from the Milo c-61-E well, these proved rather unsuccessful due to the frequent jamming off the core barrel within the Slave Point section, most probably caused by large vugs that compromised the mechanical integrity of the rock. Lost circulation problems while drilling the Sulphur Point section and the upper Keg River precluded coring in either of these two sections. Accordingly, rather than evaluating whether the Elk Point Group reservoir rocks are appropriate for CCS from an injectivity perspective, the primary focus of this core study became an assessment of the competency of the potential cap rocks within the Elk Point Group from a sealing/confinement perspective.

Weatherford Laboratories (Canada) Ltd., (Weatherford), conducted a reservoir engineering study using primarily cap rock material from the well. Specifically, pore size distribution and capillary pressure characteristics were evaluated using the mercury injection method; the characteristics of acid gas displacing equilibrium brine (drainage) and equilibrium brine displacing acid gas (imbibition) were studied along with the determination of the corresponding relative permeability curves as well as the bulk and preferential solubility of the acid gas in formation brine. Mechanical properties testing, aimed at evaluating the integrity of selected cap rock sequences, was also performed, along with the analyses of routine petrophysical parameters from representative full diameter core segments.

This report includes reservoir analyses that will allow the Fort Nelson CCS Project Team to apply the results of these laboratory studies to further its understanding of the pertinent cap rocks for each of the main injection target formations.

1.2 Conclusions and Recommendations

RPS Energy has completed a study designed to test the potential impact of acid gas ($\text{CO}_2 + \text{H}_2\text{S}$) exposure on the integrity and containment capability of several shale cap rock sequences in the Milo area of N.E. British Columbia. This study shows that when exposed to acid gas fluids (acid gas phase plus acid gas saturated brine) similar in composition to the injected acid gas fluids envisioned for the Fort Nelson sequestration project, the Ft. Simpson, Muskwa and Otter Park cap rocks retain sufficiently their high strength and sealing properties, making them competent seals for the injected acid gas fluids. This study has confirmed that the cap rock integrity should remain in excess of the requirements anticipated by the BC regulators, specifically the OGC, for the potential CCS scheme operating conditions.

The structural integrity and leak resistance of the Milo cap rock-quality shales were investigated by measuring the capillary pressures of the cap rock. In addition, the effectiveness of several potential cap rocks as containment seals was evaluated via cap rock integrity testing as well as rock mechanical testing. Several other tests undertaken during this study have assisted in the determination of the potential for leakage through the underlying aquiclude by quantifying the impact that acid gas and acid gas-saturated brine has had on the relative permeability displacement characteristics of the Lower Slave Point formation.

It was determined from the results of the series of core tests that:

1. The mercury injection capillary pressure (MICP) data indicates threshold intrusion pressures (TIPs) of 24,790 kPa (3595 psia) for the Ft. Simpson and Muskwa shales and a TIP of 6480 kPa (934 psia) for the Otter Park shale sequence. Based on the pore size distribution data, all three shale samples were comprised 100% of micropore systems with a median pore throat diameter of less than 0.01 μm . There appeared to be an excellent correlation between the TIP and the median pore size for all of the Milo c-61-E core samples (including those for the Lower Slave Point (a secondary sequestration zone) and the Lower Keg River (recognised as an aquiclude in the Fort Nelson region).
2. Each of the Ft. Simpson and Muskwa shale samples appear to be very competent cap rocks for the containment of injected acid-gas. These two shale samples were found to be totally impermeable to acid gas at injection pressures of up to 10,000 kPa. The two samples exhibited effective permeabilities to acid gas saturated brine of 4.6 nano Darcy (10^{-9} Darcy) and 0.9 nano Darcy, respectively, at injection pressures of 5500 kPa (798 psi). Both of these values are many orders of magnitude less than the commonly accepted maximum permeability to fluid of 0.001 mD.
3. Although they were sampled within 0.14 m of one another, the rock mechanical properties for the two Muskwa core samples were substantially different from one another. The average cap rock compressive strength of the two Muskwa shale samples (both tested under “as-is” conditions) was 202.75 MPa (29,400 psi). This compressive strength is significantly higher than that required to contain the expected Fort Nelson acid gas CCS project operating pressures.
4. The relative permeability measurements conducted on the two Lower Slave Point core samples indicated that the majority of the Corey exponents are reasonably low. This result suggests that the processes of acid gas displacing brine and brine displacing acid gas are equally efficient and are not likely to be subject to any significant degree of multiphase interference effects.
5. For the two c-61-E Lower Slave Point core samples, the end point relative permeability to acid gas at the irreducible brine saturation for the primary drainage cycle averaged 0.84 of the initial absolute brine permeability. This result has an obvious advantage in an acid gas sequestration operation. The irreducible brine saturation after flooding with acid gas for the two Lower Slave Point core samples averaged 0.34 and did not vary substantially between the two Milo c-61-E samples. This result indicates that approximately 0.66 of the pore space can be filled with acid gas.

The series of measureable cap rock parameters and other related data investigated in this study provide valuable information to CCS(carbon capture and storage) stakeholders, including project operators and regulators who must co-operate to establish the maximum project operating pressures

Extension of the understanding of the long-term integrity and strength of the Milo cap rocks in the presence of acid gas fluids (both brine and gas) and the demonstration that the Fort Nelson Milo Ft. Simpson, Muskwa and Otter Park cap rock integrity is not compromised when exposed to acid gas-saturated brine provides several potential benefits:

1. Regulators may allow the Fort Nelson CCS licensed operating pressures to be set relatively high (e.g. 80% of the anticipated rock fracturing pressure). This should, in turn, result in increased acid gas sequestration capacities.
2. Dissemination of this information should benefit public awareness programs.
3. Associations dealing in the accreditation of CCS sites for geological storage will be assured that injected volumes of CO₂ will remain safely sequestered over the project lifespan.

2.0 INTRODUCTION

2.1 Carbon Capture and Storage (CCS)

Disposal of acid gas, comprised of carbon dioxide (CO₂) and hydrogen sulphide (H₂S), in deep underground formations as a means for reducing atmospheric emissions of toxic and greenhouse gases produced from sour-gas reservoirs that has been practiced for over 20 years in North America. Deep saline aquifers have the largest potential storage capability and the widest distribution world-wide and consequently, represent a very large capacity for the sequestration of acid and greenhouse gases. Proper understanding the characteristics of such aquifer systems is essential in ascertaining gas injectivity and migration, and in assessing the suitability, containment, and safety of prospective injection sites

Effective CO₂ containment is achieved by the overlying tight cap rock that is initially highly saturated with formation brine, which prevents CO₂ migration into overlying strata and possibly into shallow groundwater resources. The confining properties of the cap rock are due to its very low permeability and to both relative permeability and capillary pressure effects that prevent the penetration of CO₂ into, and significant flow through the cap rock.

2.2 PCOR Partnership and Spectra Energy

The Plains CO₂ Reduction (PCOR) Partnership, led by the Energy & Environmental Research Center (EERC) at the University of North Dakota in Grand Forks, North Dakota, is one of seven regional partnerships operating under the U.S. Department of Energy (DOE) National Energy Technology Laboratory (NETL) Regional Carbon Sequestration Partnership (RCSP) Program. The RCSP Program is a government–industry effort tasked with determining the most suitable technologies, regulations, and infrastructure needs for CCS on the North American continent.

As part of its Phase III activities, the PCOR Partnership is currently assessing the feasibility of injecting significant quantities of CO₂ near the Fort Nelson Gas Processing Facility in northeastern British Columbia, Canada. The PCOR Partnership will conduct a modeling and monitoring, mitigation, and verification (MMV) program associated with a project that plans to inject approximately 1.2 million tons of CO₂ per year. Spectra Energy, the operator of the Fort Nelson gas plant, is working closely with the British Columbia Ministry of Energy, Mines, and Petroleum Resources (BCMEMP) to obtain the necessary permits and regulatory approval to conduct large-scale CO₂ injection activities in the area.

2.3 Fort Nelson CCS Project Area

Spectra's sour CO₂ injection plan calls for injection into the highly porous and permeable Sulphur Point formation found at a depth of between 2000 and 2500 m. The lower Keg River formation may also be considered for potential acid gas injection at a later date. Formations in this depth range are expected to be at temperatures and pressures that ensure the injected CO₂ remains in a supercritical state. The thickest, most comprehensive seal for the Devonian carbonate rock formations under consideration will be provided by the massive and extensive shales of the Fort Simpson Formation. Based on the very low permeability as well as the high geomechanical strength anticipated for this shale, the Fort Simpson cap rock is expected to provide a very competent seal for injection into the underlying brine reservoirs. An additional potential cap rock, the Muskwa shale, was also evaluated during this study.

During 2009, Spectra drilled the first Fort Nelson CCS test well at Milo c-61-E/94-J-10. The well penetrated into the top of the Slave Point / Sulphur Point and Keg River carbonate barrier reef

complex. Spectra ran a series of well evaluation logs and in addition, cored part of the Fort Simpson and Muskwa shales before running and setting the intermediate casing at 2,040 m MD.

The log evaluation program indicated that the Ft Simpson and Muskwa shales form a cap rock that is a total of 557.7 m in thickness and hence, comprise a very thick seal for the underlying Sulphur Point saline reservoir.

After intermediate casing was set in the c-61-E well, drilling and subsequently, coring activities were conducted to a total depth of 2561 m into the Chinchaga quartzite. Although numerous coring attempts were made, the core recovery in the lower section of the well was poor owing to the many vugs and fractures encountered in the Slave Point and Sulphur Point formations. Appendix 1, extracted from Reference 1, contains more details of the repeated coring attempts and the numerous difficulties encountered.

Below the base of the Muskwa, there is a 32 m thick Otter Park section that appears to be a tight dolomite (petrophysical evaluation identified a few streaks of porosity totaling some 2.5 m of net pay (using 3% porosity cut-off) but the streaks do not appear to be connected). This unproductive Otter Park should provide additional containment at the Milo c-61-E location.

2.4 Properties of Cap Rock

A competent cap rock is characterised as having high compressive strength, so as to be physically resistant to the in-situ reservoir pore pressure. In addition, the confining properties of the cap rock are due to its very low permeability and to relative permeability and capillary pressure effects that prevent the penetration of acid gas into, and significant flow through the cap rock. Breakdown of the cap rock could result from the injection of fluids in excess of the fracture resistance or strength of the cap rock leading to potentially significant leakage. Some degree of fluid leakage or seepage could also be caused by exceeding the threshold intrusion pressure (capillary breakthrough). If the cap rock is not naturally fractured, the necessary condition to avoid acid gas leakage is to maintain the injection pressure below the capillary entry pressure or the rock fracturing pressure, whichever is lower. Even if the injected acid gas pressure is higher than the capillary entry pressure (but lower than the rock fracturing pressure), if the absolute and relative permeabilities of the cap rock are sufficiently low, then the acid gas may percolate through the cap rock on only a geological time scale, and thus may still be insignificant from an operational and acid gas storage perspective. Consequently, it is very important to determine the acid gas-brine displacement characteristics and capillary entry pressure of the confining cap rocks of deep saline aquifers.

Industry accepted design criteria have been established for both gas storage reservoirs and sour gas disposal reservoirs. A competent cap rock should optimally have a Threshold Injection Pressure (TIP) that exceeds 7,000 kPa (1,000 psi), combined with an absolute liquid permeability of 1 nano Darcy (10^{-9} D) (**References 2 and 3**). In practice, an absolute liquid permeability of 0.001 mD is typically recognised as the highest acceptable cap rock permeability, and lower values of TIP may be acceptable as long as the absolute permeability is low enough and other project parameters such as pressure, fluid type and cap rock quality are within reasonable margins. This is usually determined on an individual application (site) basis, through a risked project analysis.

The structural integrity and leak resistance of the Milo cap rock-quality shales were investigated by measuring the **Capillary Pressures** of the cap rock. Several tests undertaken during this

study have assisted in determining the potential for leakage through the underlying aquiclude* by quantifying the impact that acid gas and acid gas-saturated brine has had on the **Relative Permeability** displacement characteristics of the Lower Slave Point formation. Most importantly, the effectiveness of several potential cap rocks as containment seals was evaluated via **Cap Rock Integrity** testing as well as **Rock Mechanical** testing.

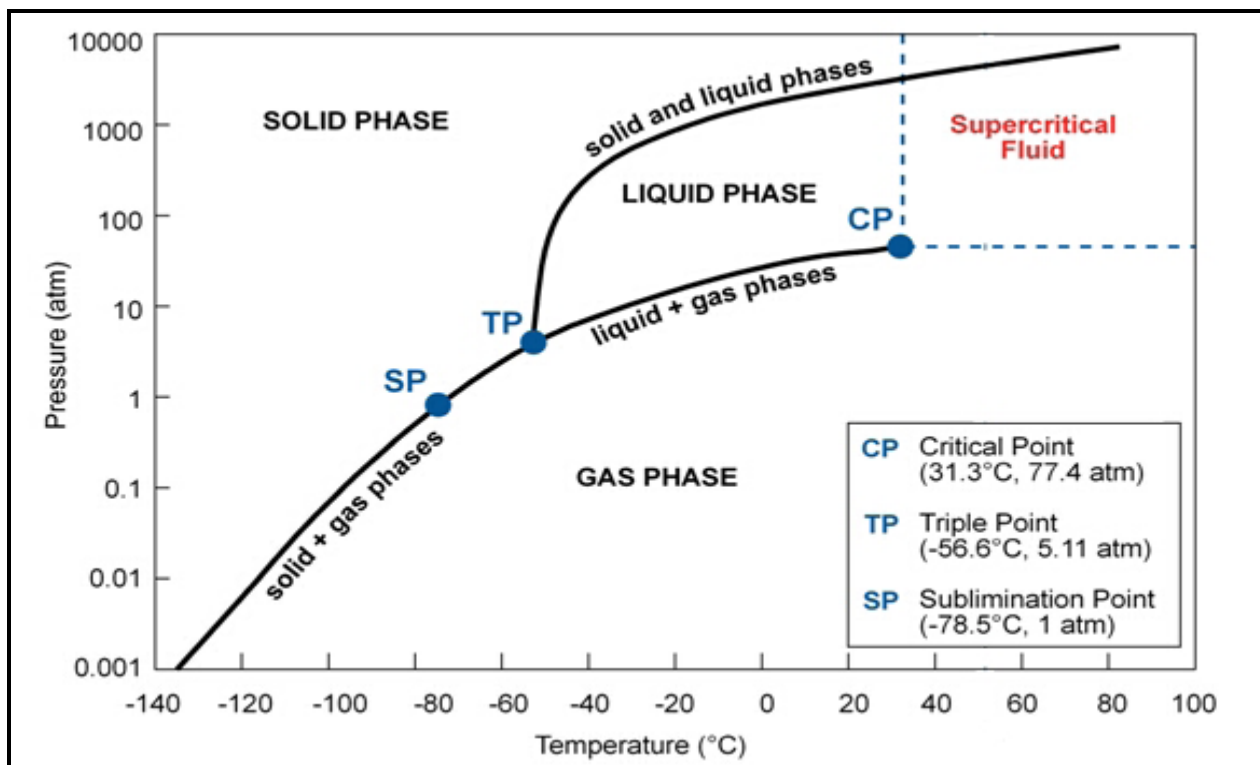
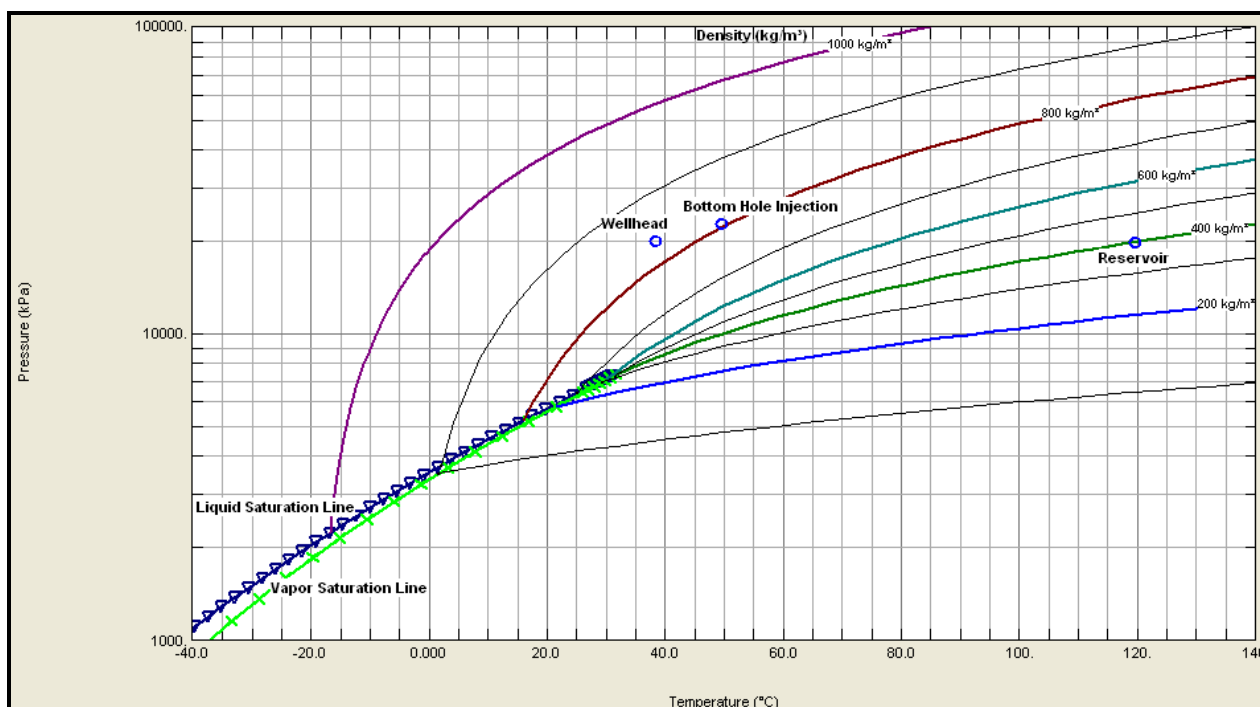
2.5 Properties of Milo Acid Gas

The composition of the acid gas stream from the Fort Nelson gas plant, at least for the year 2012, is anticipated to be 95% CO₂ along with 4.4% H₂S. These two components make up roughly 99.4% of the acid gas stream with the balance represented by N₂ (0.11%) and methane (0.49%).

The pressure-volume-temperature (PVT) nature of CO₂ and acid gas fluids is complex. **Figure 2-1** shows a schematic of CO₂ typical PVT behaviour. Potential phase behaviour problems can occur frequently downhole in an acid gas disposal operation. Depending on the downhole injection pressure and temperature conditions, the injected acid gas could be a miscible supercritical fluid or be both immiscible liquid and vapour gas phases in the near wellbore region with adverse relative permeability and injectivity performance impact. As such, the allowable pressure is a very important parameter that can impact operating costs as well as injection well performance.

Figure 2-2 and **Figure 2-3**, generated with REFPRO, a fluid property calculation software, illustrate complex phase behaviour of the Milo acid gas mixture with temperature and pressure as the acid gas (95% CO₂, 4.4% H₂S, 0.11% N₂ and 0.49% CH₄) changes phase. As a supercritical fluid, also referred to as “dense” phase, the acid gas is in a monophasic condition which is operationally favourable for injection. It is thus desirable to operate at pressures with a good safety margin above the critical point as small changes in temperature and pressure can result in large changes in density.

* An **aquiclude** (or aquifuge) is defined as a hydrogeological unit that comprises a solid, impermeable interval underlying or overlying an aquifer.

Figure 2-1: PVT Behaviour of CO₂Figure 2-2: Milo Acid Gas (CO₂ 95%, H₂S 4.4%, N₂ 0.11%, C1 0.49%) Pressure vs Temperature

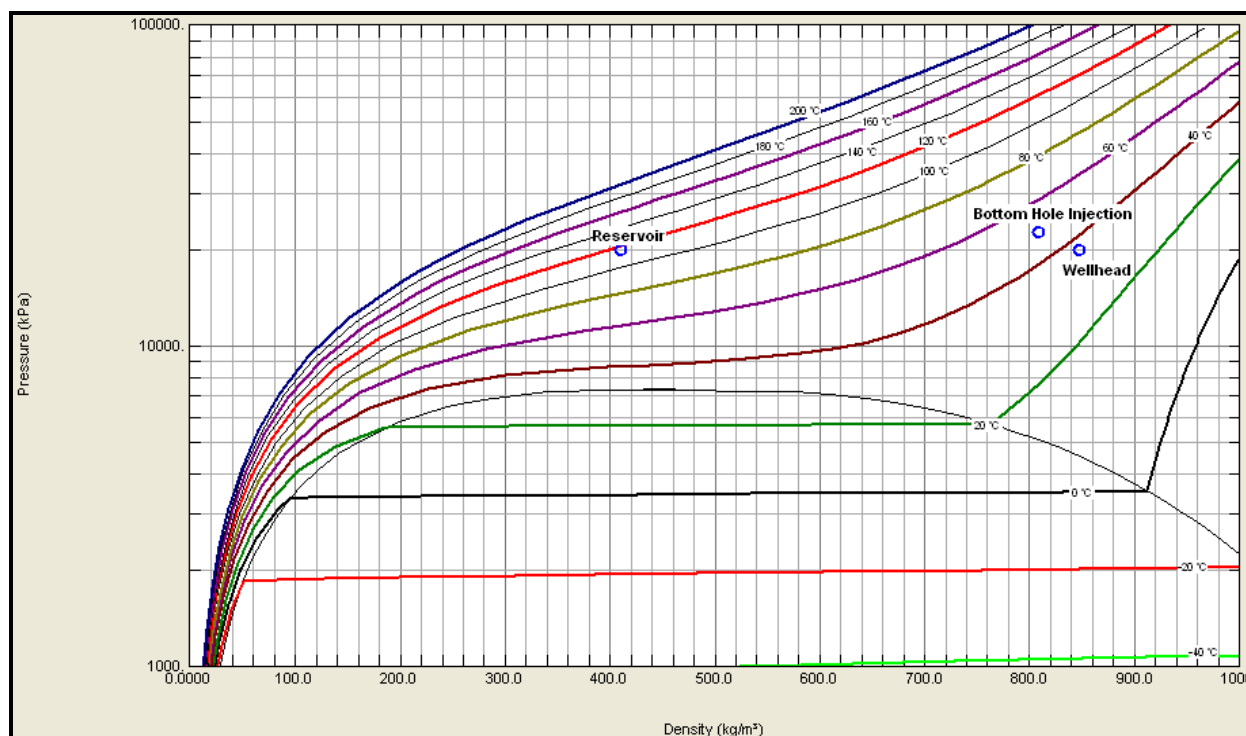
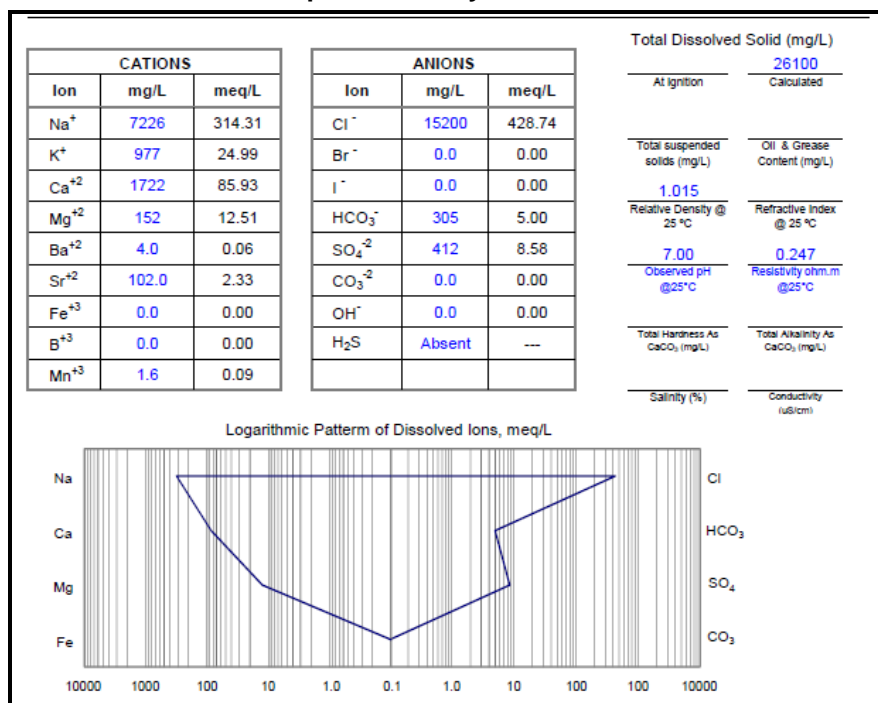


Figure 2-3: Milo Acid Gas (CO₂ 95%, H₂S 4.4%, N₂ 0.11%, C1 0.49%) Pressure vs Density

2.6 Composition of Milo Equilibrium Brine

The composition of the synthetic brine required for the cap rock integrity and relative permeability testing was provided by Spectra Energy as is detailed in **Table 2-1**, below.

Table 2-1: Composition of Synthetic Formation Brine



2.7 Core Sample Selection and Preparation

Spectra Energy supplied Weatherford Laboratories with the cores from the SECCS c-61-E / 94-J-10 well in the Milo area of NE BC. The cores represented various formations as follows:

Interval: 2027.60 m - 2039.40 m	Formation: Lower Ft. Simpson
Interval: 2040.50 m - 2058.60 m	Formation: Muskwa & Otter Park
Interval: 2129.00 m - 2143.20 m	Formation: Lower Slave Pt.
Interval: 2362.20 m - 2387.80 m	Formation: Lower Keg River

All of the cores were received in a non-preserved state. It should be noted that all of the depths shown in both this report and the Weatherford Laboratories report (Reference 4) are the measured core depths; these depths may not correlate precisely with the well log depths as there were not a sufficient number of markers in the Muskwa shale and Devonian reef sections to accurately adjust the core to the well log depths.

Selected full diameter samples were cut from the Ft. Simpson and Muskwa formations for cap rock evaluation and from the Lower Slave Pt. and Lower Keg River formations for the gas/brine relative permeability testing. It is noted that sample REL K-3 from the Lower Keg River formation, originally selected for relative permeability testing was cancelled by RPS Energy. Companion sample chunks, each less than 1" diameter and 1" long, adjacent to the cap rock integrity and relative permeability test samples were subjected to capillary pressure testing using the mercury injection method.

The initial test program also called for plug samples to be taken from the Ft. Simpson formation, the Muskwa formation as well as the Lower Slave Pt. formation for mechanical properties testing. Due to the very fissile nature of the shale core in the Ft. Simpson and Lower Slave formations, it was not possible to obtain the competent plug samples needed for these measurements. After over 30 unsuccessful attempts with various methods of drilling the samples (including high pressure water jet - plasma cutting), this portion of the planned study was cancelled. (Photos of these attempts are shown in Appendix 2 for reference). However, two 2.54 cm (1") samples were successfully recovered from the Muskwa formation and were subjected to mechanical properties testing at Weatherford Labs in Houston, Texas.

Table 2-2 provides a listing of the depths as well as a description of the type of core testing completed of each core sampled from the Milo c-61-E well. This Table also indicates the formation name as well as the size of core sample (1" plug or full diameter core) used for each specific core test. Appendix 3 contains photos of all of the core samples using the same sample labels as provided in **Table 2-2** (e.g. MICP-1A). It should be noted that these photos were taken prior to cutting the core plugs and full diameter samples. Consequently, as described above, due to sampling difficulties, some of the sample depths may not precisely correspond to the actual point at which the sample was removed but the intended and actual depths should still be relatively close to one another. Unfortunately, no core photos after the core plugs were taken are available from Weatherford Laboratories.

Figure 2-4 is a schematic diagram showing the relative depths of each of the various core samples in relation to one another and also to the three successful drillstem tests (DSTs) that were conducted in the Milo c-6-E well in May, 2009. The results of the analyses of these three

DSTs are detailed in Reference 5, a CCS tenure application submitted by Spectra Energy to British Columbia Titles, and will not be covered in this report that deals primarily with the properties of the Milo c-61-E cap rocks (Ft. Simpson, Muskwa and Otter Park) as well as the non-reservoir aquicludes (Lower Slave Point and Lower Keg River).

Table 2-2: Summary of All Milo c-61-E Core Test Sample Depths

Final Weatherford Sample Listing					
Sample I.D.	Depth (m)	Core #	Box #	Formation	Sample Description
<i>Top of Core</i>	<i>2027.60</i>				
TH1*	2030.04	1	3	Lw Ft Simpson	Sample chunks (150g) for Dr. Ernie Perkins
CR-1A	2031.0 - 2031.05	1	3	Lw Ft Simpson	Cut full 4" diameter section for Cap Rock testing, CR-1A: 2031.00-2031.05m
TS1-A	2031.06	1	3	Lw Ft Simpson	& second chunk for Thin Section Petrology, approx 50 g
MICP-1A	2031.06	1	3	Lw Ft Simpson	Take small chunk (less than 1 inch cube) for MICP
<i>Bottom of Core</i>	<i>2039.40</i>				
<i>Top of Core</i>	<i>2040.50</i>				
T1*	2042.12	3	2	Muskwa	Sample chunks (150g) for Dr. Ernie Perkins
T3*	2045.75	3	4	Muskwa	Sample chunks (150g) for Dr. Ernie Perkins
MP1:	2045.67-2045.70	3	4	Muskwa	1" Plug Vertical MP1: 2045.67-2045.70;
MP2:	2045.81-2045.85	3	4	Muskwa	1" Plug Vertical MP2: 2045.81-2045.85;
CR-2A	2048.0 - 2048.1	3	6	Muskwa	Cut full diameter section for Cap Rock testing, 2048.00-2048.10m
TS2	2048.11	3	6	Muskwa	& second chunk for Thin Section Petrology, approx 50 g
MICP-2	2048.11	3	6	Muskwa	Take small chunk (less than 1 inch cube) for MICP
TS3	2049.50	3	7	Muskwa / Otter Park	Drill 1 inch plug, cut 3/4" long portion for MICP, the rest for petrology
MICP-3	2049.50	3	7	Muskwa / Otter Park	Drill 1 inch plug, cut 3/4" long portion for MICP, the rest for petrology
<i>Bottom of Core</i>	<i>2058.60</i>				
<i>Top of Core</i>	<i>2129.00</i>				
TS4	2129.16	4	1	Lower Slave Pt.	Sample chunk for Petrology
TS5	2130.00	4	1	Lower Slave Pt.	Sample chunk for Petrology
MICP-4	2130.01	4	1	Lower Slave Pt.	Drill 1 inch plug nearby and cut 3/4 inch for MICP
REL K-1	2130.02 - 2130.13	4	1	Lower Slave Pt.	Cut full diameter 2.5" sample for Rel Perm Test. 2130.02-2130.13m
CR1	2139.08	5	1	Lower Slave Pt.	
REL K-2	2139.08 - 2139.15	5	1	Lower Slave Pt.	Cut full diameter 2.5" sample for Rel Perm Test. 2139.08-2139.15m
TS6	2140.83	5	2	Lower Slave Pt.	Sample chunk for Petrology
TS7	2143.27	6	1	Lower Slave Pt.	Sample chunk for Petrology
<i>Bottom of Core</i>	<i>2143.20</i>				
<i>Top of Core</i>	<i>2362.20</i>				
TS8	2362.64	8	1	Lower Keg River	Sample chunk for Petrology
REL K-3	2362.71-2362.76	8	1	Lower Keg River	Cut full diameter 2.5" sample for Rel Perm Test. 2362.71-2362.76m
MICP-5	2362.70	8	1	Lower Keg River	Drill 1 inch plug nearby and cut 3/4 inch for MICP
TS9	2363.70	8	1	Lower Keg River	
TS10	2387.00	9	1	Lower Keg River	Sample chunk for Petrology
<i>Bottom of Core</i>	<i>2387.80</i>				
* Although samples TS3 and MICP-3 were reported to be taken at the same depth, it is apparent that TS-3 sampled a dolomite section whereas MICP-3 corresponds to a shale.					

Prior to testing, all the core samples underwent azeotropic cleaning with chloroform and methanol to remove any residual fluid saturation.

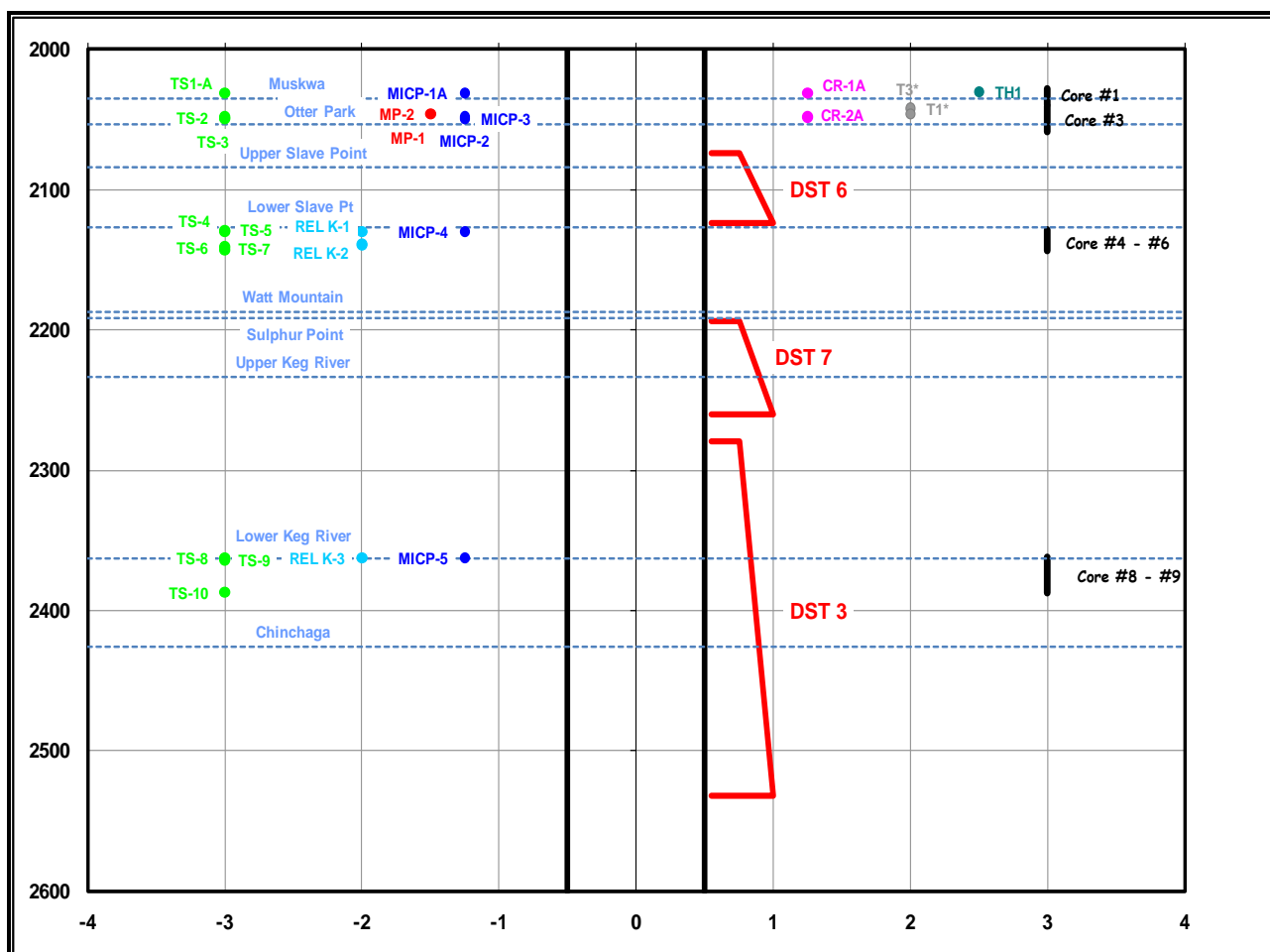


Figure 2-4: Schematic Diagram of All Milo c-61-E Core Samples and DST Intervals

As noted in **Table 2-2**, only three full diameter core samples, two from the Lower Slave Point and one from the Lower Keg River section were recovered. The routine core measurements from these three cores are summarised in **Table 2-3**.

The analyses of the ten thin sections identified in **Table 2-2** and **Figure 2-4** were completed in a separate report prepared by Graham Davies (Reference 6) and will not be addressed in this report.

Table 2-3: Summary of Routine Core Parameters

SUMMARY OF PHYSICAL CORE PARAMETERS								
SECCS MILO c-61-E/94-J-10								
Sample I.D.	Top Depth (m)	Length (cm)	Porosity (fraction)	Air Permeability			Grain Density (kg/m3)	Bulk Density (kg/m3)
				Kmax (mD)	K90 (mD)	Kvert (mD)		
*CR-1A	2031.00	8.17	0.033	3.78	1.44	0.03	2740	2650
*CR-2A	2048.00	10.2	0.026	5.40	2.10	1.10	2660	2590
REL K-1	2130.02	8.32	0.066	2.10	1.50	0.29	2820	2640
REL K-2	2139.08	8.90	0.031	2.30	0.16	1.10	2820	2730
REL K-3	2362.71	10.9	0.024	0.17	0.11	0.12	2810	2750
*REL K-1	2130.02	8.32	0.032	1.90	0.51	0.30	2790	2700
*REL K-2	2139.08	8.90	0.031	0.43	0.16	0.34	2810	2770

NOTE * represents the routine porosity and permeability measured on post test samples.

3.0 MERCURY INJECTION CAPILLARY TESTING

Five intervals were selected for Mercury Injection Capillary Pressure (MICP) testing. The samples were chosen so as to include each of the main formations encountered in the Milo c-61-E well: specifically, the Ft. Simpson, Muskwa, Otter Park, Lower Slave Point and Lower Keg River intervals. With the exception of the Otter Park, the selected samples were either small chunks (less than 1 inch cubes) or 0.75 inch plugs taken from the parent vertical full diameter cores that had previously been selected for either cap rock testing or relative permeability testing. The plug samples were drilled in a vertical orientation so that the permeability would be measured along the vertical axis (perpendicular to the natural bedding planes)) to mimic the direction of potential fluid penetration in the reservoir cap rock.

Prior to subjecting the samples to mercury injection capillary testing, the individual samples were cleaned using an azeotropic mixture of chloroform and methanol to remove any hydrocarbons and brine in the samples. Then, using a Micromeritics Autopore 9220 instrument, capillary pressure data was generated to a maximum mercury intrusion pressure of 414 MPa (60,000 psia). For each sample, the measured data, fully documented in **Reference 4**, included the wetting phase saturation, the capillary pressure, the pore throat diameter and the height of the transition zone (for an equivalent air-water system).

Figure 3-1 provides a plot of the pore size distributions for each of the 5 samples tested. The air-water capillary pressure curves at reservoir conditions (converted from the measured air-mercury capillary pressure data) for each of the 5 subject samples are documented in Reference 4. The pore size distribution statistics as well as the threshold intrusion pressure (TIP) for each of the 5 test samples is presented in **Table 3-1**. In this table, the pore throat size distribution was divided into the following three categories to further characterise rock matrix: Micropores - less than 3 microns in diameter; Mesopores - between 1 to 3 microns in diameter and Macropores - greater than 3 microns in diameter.

Table 3-1: Pore Size Distribution and TIP Values

Sample I.D.	Depth (m)	Median Pore Throat Size (µm)	Pore Throat Types			Threshold Intrusion Pressure (kPa)	Formation
			Micropores Pore Diam < 1 micron	Mesopores Pore Diam 1-3 microns	Macropores Pore Diam > 3 microns		
1A	2031.06	0.01	100.0%	0.0%	0.0%	24,970	Ft. Simpson
2	2048.11	0.01	100.0%	0.0%	0.0%	24,970	Muskwa
3	2049.5	0.01	100.0%	0.0%	0.0%	6480	Otter Park
4	2130.01	3.62	26.8%	22.5%	50.7%	35	Lower Slave Pt.
5	2362.7	0.18	96.1%	3.9%	0.0%	791	Lower Keg River
Low k		0.60	71.4%	9.0%	19.6%	355	Albeta Carbonate
Mid k		8.36	22.9%	10.6%	66.5%	32	Albeta Carbonate
High k		16.4	14.7%	9.0%	76.3%	17	Albeta Carbonate
Colorado Gp Shale		0.011	96.1%	3.9%	0.0%	172	Colorado Gp Shale
Calmar Shale		0.006	96.1%	3.9%	0.0%	72,827	Calmar Shale
Wabamun #1		0.645	8.1%	18.9%	1.0%	494	Wabamun

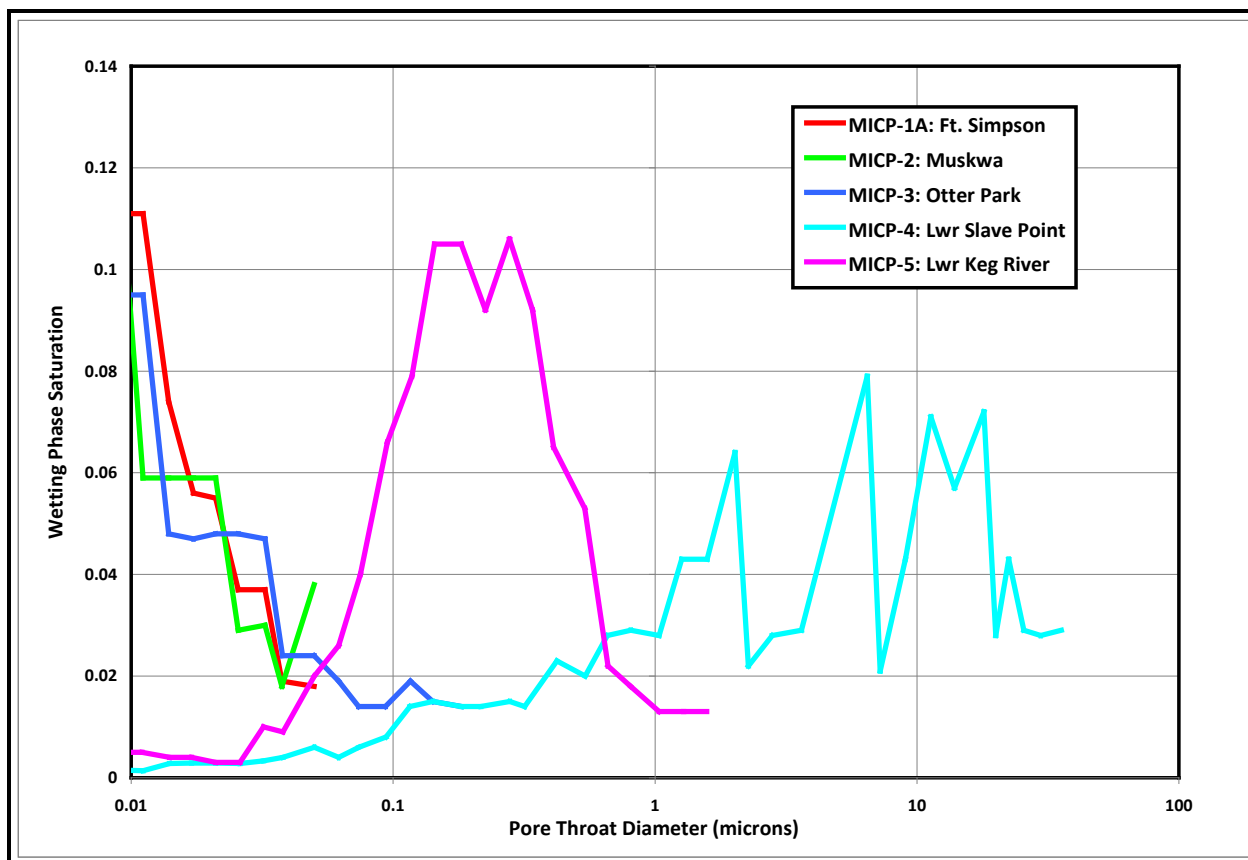


Figure 3-1: Milo c-61-E Samples Pore Size Distribution

As shown in **Table 3-1**, the threshold intrusion pressure and the pore size data for the three shale samples: Ft. Simpson, Muskwa and Otter Park, indicate ultra fine grained matrices with 100% microporosity and with average pore throat diameters of less than 0.01 micron.

In contrast, the Lower Slave Point sample was dominated by macroporosity (over 50% of pore throats are over 3 microns in size). With a threshold intrusion pressure of only 35 kPa (5.1 psi), this zone is considered to be a secondary reservoir/storage zone (after the primary Sulphur Point formation from which no viable core samples were recovered). Finally, the MICP data for the Lower Keg River formation exhibited over 96% microporosity as well as a threshold intrusion pressure of 791 kPa (115 psi), much lower than any of the three shale samples but considerably higher than the TIP for the Lower Slave Point sample. This result would indicate the storage capacity of the Lower Keg River interval is much poorer than the Lower Slave Point zone and is consistent with the fact that the Lower Keg River is not considered to be a feasible reservoir/storage interval in the Milo area.

The pore scale flow characteristics, including the average size and threshold capillary pressure of three different permeability groupings of carbonate rocks (as detailed in **Reference 7**), as well as two shale sequences for which laboratory data are available (**Reference 8**) are also summarised at the base of **Table 3-1**. The Wabamun #1 sample mercury injection capillary pressure results, also taken from Reference 6, have also been included in this table since this reservoir rock appears to be most comparable to the Milo c-61-E Lower Slave Point core sample.

The low, mid and high permeability carbonate groups shown in these tables represent carbonate rocks with permeabilities in the mD, tens of mD and hundreds of mD ranges, as categorised below:

- Group 1 - Low permeability carbonates (< 10 mD effective initial absolute permeability to brine)
- Group 2 - Mid range permeability carbonates (10-100 mD effective initial absolute permeability to brine)
- Group 3 - High permeability carbonates (> 100 mD effective initial absolute permeability to brine)

Based on these definitions, the MICP-4 Lower Slave Point core sample from the Milo c-61-E well, with an estimated air permeability of 1.9 mD (from the REL K-1 sample taken at the same depth), would represent a “low” permeability carbonate.

Figure 3-2 illustrates the reasonably good correlation between the threshold injection pressure and the (logarithm of) the median pore size for the Otter Park, Lower Slave Point and Lower Keg River sections. Also shown on this plot are the TIPs and median pore size for the additional carbonate samples taken from Reference 7.

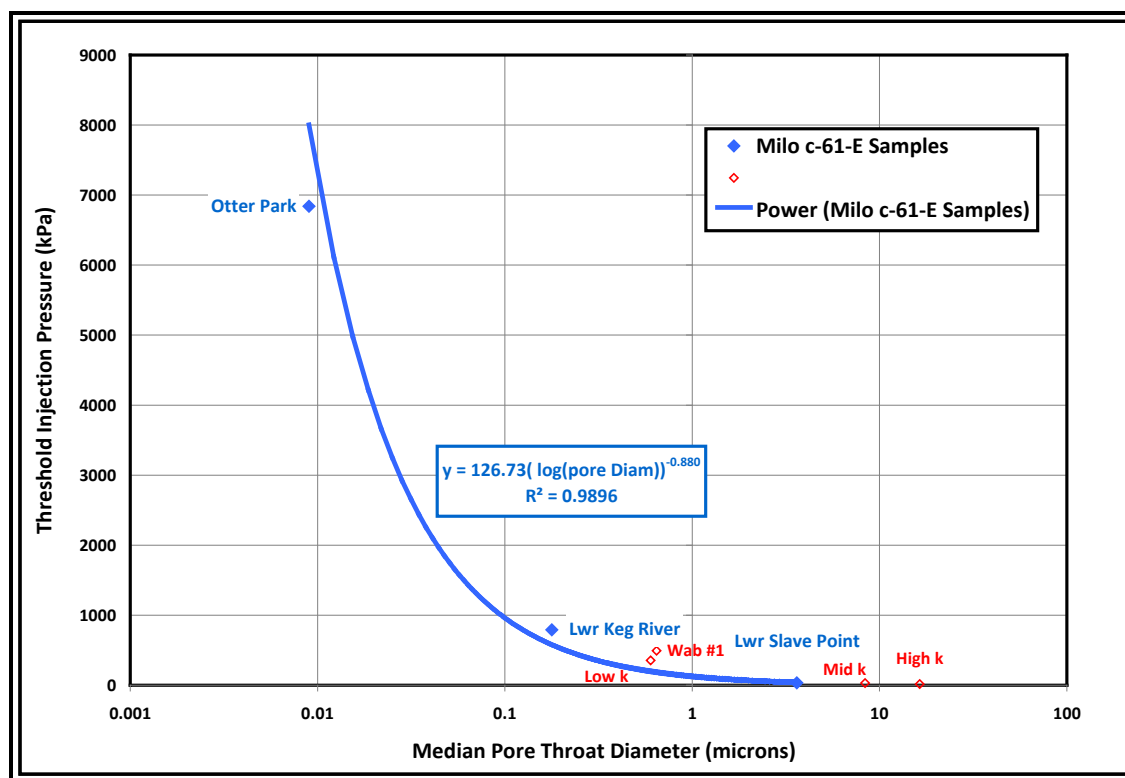


Figure 3-2: Threshold Injection Pressure versus Median Pore Size

4.0 ROCK MECHANICS

4.1 Mechanical Testing

To evaluate the impact of acid gas exposure on the Muskwa shale cap rock, the rock mechanical properties, specifically the triaxial compressive strength and the dynamic elastic parameters were determined using two representative sample plugs cut approximately 0.14 m apart. The Triaxial Compressive Strength test involves loading each cylindrical core plug axially to failure, at constant confining pressure; the peak value of the axial stress is taken as the confined compressive strength of the plug. In addition to axial stress, axial and radial strains were monitored during this test to determine the basic (static) elastic constants. Dynamic elastic constants were also determined by measuring the acoustic wave velocities in the plugs.

Weatherford drilled two 1 inch OD vertical core plugs from the full diameter Muskwa core shown in **Figure 4-1**. Both core samples were tested under “as-is” conditions. All sample plugs were examined by white light and CT scan to confirm that there were no existing or drilling induced flaws that would skew the measured strength parameters.

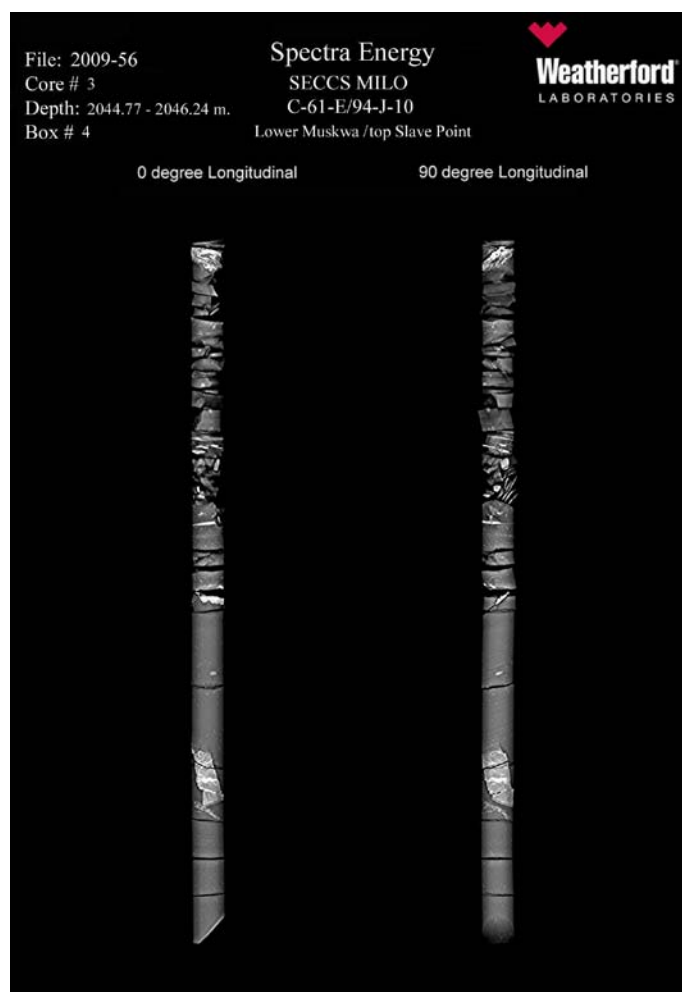


Figure 4-1: CT Scan of Muskwa Core Intervals

The Rock Mechanics Testing was carried out by Weatherford Laboratories in Houston, Texas as per the following general test procedure;

1. Two right cylindrical plugs were cut from the full diameter core and their ends ground parallel to each other within 0.001 inch. A length to diameter ratio of 2:1 was utilised to obtain representative mechanical properties. The physical dimensions and weight of the specimen were recorded.
2. The specimen to be tested was placed between two end-caps and a heat-shrink jacket was placed over the specimen.
3. Axial strain and radial strain devices were mounted in the end-caps and on the lateral surface of the specimen, respectively.
4. The specimen assembly was placed into the pressure vessel and the pressure vessel was filled with hydraulic oil. Confining pressure was increased to the desired hydrostatic testing pressure, in the case of the single stage triaxial compressive strength test, or to the first-stage hydrostatic testing pressure, in the case of the multi-stage triaxial compressive strength test.
5. The ultrasonic velocities were measured at the hydrostatic confining pressure.
6. The specimen assembly was then brought into contact with a loading piston that allows application of axial load. The axial load was increased at a constant displacement rate until the specimen fails while the confining pressure was held constant (single stage triaxial compressive strength test) or to the near-peak stress level while the confining pressure is held constant at the next specified hydrostatic testing stage (multi-stage triaxial compressive strength test).
7. The axial load was increased at a constant displacement rate until the specimen failed while the confining pressure was held constant at the final stage (for the multi-stage triaxial compressive strength test).
8. The axial stress was reduced to the initial hydrostatic condition after the sample failed.
9. The confining pressure was reduced to zero and the sample was disassembled.

The rock mechanics testing included the Compressive Strength analysis tests, the measurement of the Compressional and Shear Wave Velocities as well as the analysis of the Static and Dynamic Young's Modulus and Poisson's Ratio as well as the Bulk and Shear Moduli. The properties derived from the tests measuring the strain for a given applied stress, are static elastic constants. Dynamic elastic constants were determined by measuring compressional and shear sound wave velocities through the material. Dynamically measured moduli are more accurate than the static moduli since the latter are affected by contributions to strain from test equipment deflection or other material properties. Appendix 4 provides a technical overview of the measured elastic parameters. The competence of a cap rock or indeed any structural material is often simplistically ranked by its measured compressive strength. However, the strength of a material is complex and is related not only to the compressive strength but to how its dimensions respond to applied forces; this is determined by Young's Modulus of elasticity and Poisson's Ratio.

The axial stress is determined by dividing the measured load by the initial cross-sectional area of the specimen. Differential axial stresses are plotted against both axial strain ϵ_L ($= \Delta L/L_o$, where L_o is the initial length and ΔL is the length change) and radial strain ϵ_R ($= \Delta D/D_o$, where D_o is the initial diameter and ΔD is the diameter change). Differential stress (σ_d) is defined as

the difference between the total axial stress (σ_1) and the confining pressure (P_c). For the sign conventions, compressive stress and contraction (shortening) are considered positive. Therefore, positive axial strain indicates a shortening of the specimen length and negative radial strain indicates an increase of the specimen diameter during the test.

Table 4-1 provides a summary of the static and dynamic elastic constants for the two individual Muskwa shale samples. **Figure 4-2** and **Figure 4-3** display the results from the single and the multi-stage triaxial compressive strength tests, respectively, completed on the two Muskwa shale samples. The multi-stage compressive strength test completed on sample MP2 was conducted at confining pressures of 2.07 MPa, 10 MPa and 17.93 MPa (300 psi, 1,450 psi and 2,600 psia).

The compressive strength of the two Muskwa specimens that is presented in **Table 4-1** is the maximum total stress during the test. The static Young's modulus (E_s) is determined by the linear-least-squares slope of the linear part of the differential stress versus the axial strain curve. Likewise, the static Poisson's ratio (ν_s) is determined by the linear-least-squares slope of the radial strain versus the axial strain curve over the same interval as the Young's modulus was determined. For the two Muskwa samples, the values for Young's modulus and Poisson's ratio were determined at a stress level that was between 40% and 50% of the maximum differential stress.

Table 4-1: Summary of Static and Dynamic Elastic Constants

Sample No.	Depth (m)	Confining Pressure (MPa)	Compressive Strength (MPa)	Static Young's Modulus (MPa)	Static Poisson's Ratio
MP1	2045.67	17.93	173.97	34780	0.22
MP2	2045.81	17.93	231.53	44915	0.27

Sample No.	Depth (m)	Confining Pressure (MPa)	Bulk Density (g/cc)	Ultrasonic Velocity		Dynamic Elastic Parameter			
				Vp (km/sec)	Vs (km/sec)	Young's Modulus (GPa)	Poisson's Ratio	Bulk Modulus (GPa)	Shear Modulus (GPa)
MP1	2045.67	17.93	2.73	4.51	2.79	50.49	0.19	27.32	21.18
MP2*	2045.81	17.93	2.76	5.26	3.28	70.06	0.18	36.80	29.62

* velocities determined with 6.9 MPa differential stress

As shown in the preceding table, the triaxial compressive strength of sample MP1 was 173.97 MPa (25,232 psi) at the maximum confining pressure of 17.93 MPa (2,600 psi) with a static Young's modulus of 34,780 MPa (5,044,400 psi) and a static Poisson's ratio of 0.22. The acoustic velocities were determined for sample MP1 at the 17.93 MPa (2,600 psi) confining pressure were 4.51 km/sec and 2.79 km/sec for the compressional and shear waves, respectively. The dynamic Young's modulus and Poisson's ratio, determined from the acoustic velocities and the bulk density of the sample were 50.49 GPa (7,323,000 psi) and 0.19, respectively.

The triaxial compressive strength of sample MP2, determined at a confining pressure of 17.93 MPa (2,600 psi) during the multi-stage triaxial test was 231.53 MPa (33,580 psi). The static Young's modulus was measured as 44,915 MPa (6,514,000 psi); the static Poisson's ratio was 0.27. The acoustic velocities determined for sample MP2 at the 17.93 MPa (2,600 psi) confining pressure with a differential stress of 6.9 MPa (1,000 psi) were 5.26 km/sec and 3.28 km/sec for the compressional and shear waves, respectively. The dynamic Young's modulus and Poisson's ratio, determined from the acoustic velocities and the bulk density of the sample were 70.06 GPa (10,161,000 psi) and 0.18, respectively.

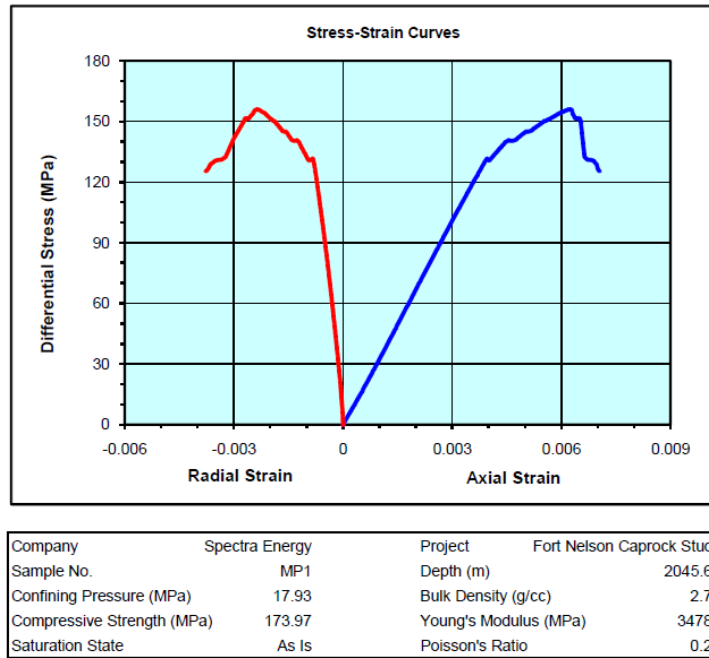


Figure 4-2: Single Stage Triaxial Compressive Strength Test on Sample MP1

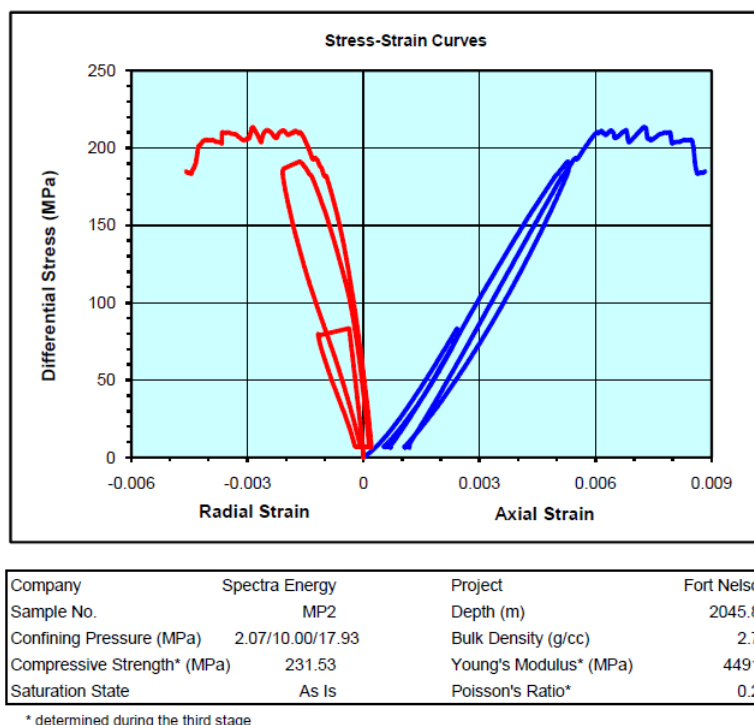


Figure 4-3: Multi-Stage Triaxial Compressive Strength Test on Sample MP2

The two samples show different mechanical properties although the two samples were taken within 0.14 m of one another. The compressive strength and static Young's modulus of sample MP2 are approximately 30% higher than those of sample MP1. This higher strength and Young's modulus are also reflected in the compressional and shear wave velocities. The acoustic velocities of sample MP2 are higher than those of sample MP1 by roughly 17%. The dynamic Young's moduli of both samples are higher than the static Young's moduli, as is observed for most of the sedimentary rocks. Sample MP2 was slightly more calcareous and its density was slightly higher than sample MP1.

A Mohr-Coulomb failure analysis was also performed on the MP2 Muskwa sample using the compressive strengths obtained from the multi-stage triaxial test, to determine the angle of internal friction, cohesion and the unconfined compressive strength.

The total compressive strengths from each stage of the triaxial compressive strength test were plotted against confining pressure; Mohr semicircles were constructed and the Mohr-Coulomb failure envelope was subsequently fit to the Mohr semicircles. The internal angle of friction for sample MP2 was determined as 53.5 degrees, corresponding to a coefficient of internal friction of 1.35. The intrinsic cohesion was 13.3 MPa (1,929 psi) with the corresponding unconfined compressive strength of 80.7 MPa (11,7000 psi).

Figure 4-4 on the following page, illustrates the results of the Mohr-Coulomb failure analyses that were conducted on the Milo c-61-E Muskwa MP-2 sample at 2045.81 m.

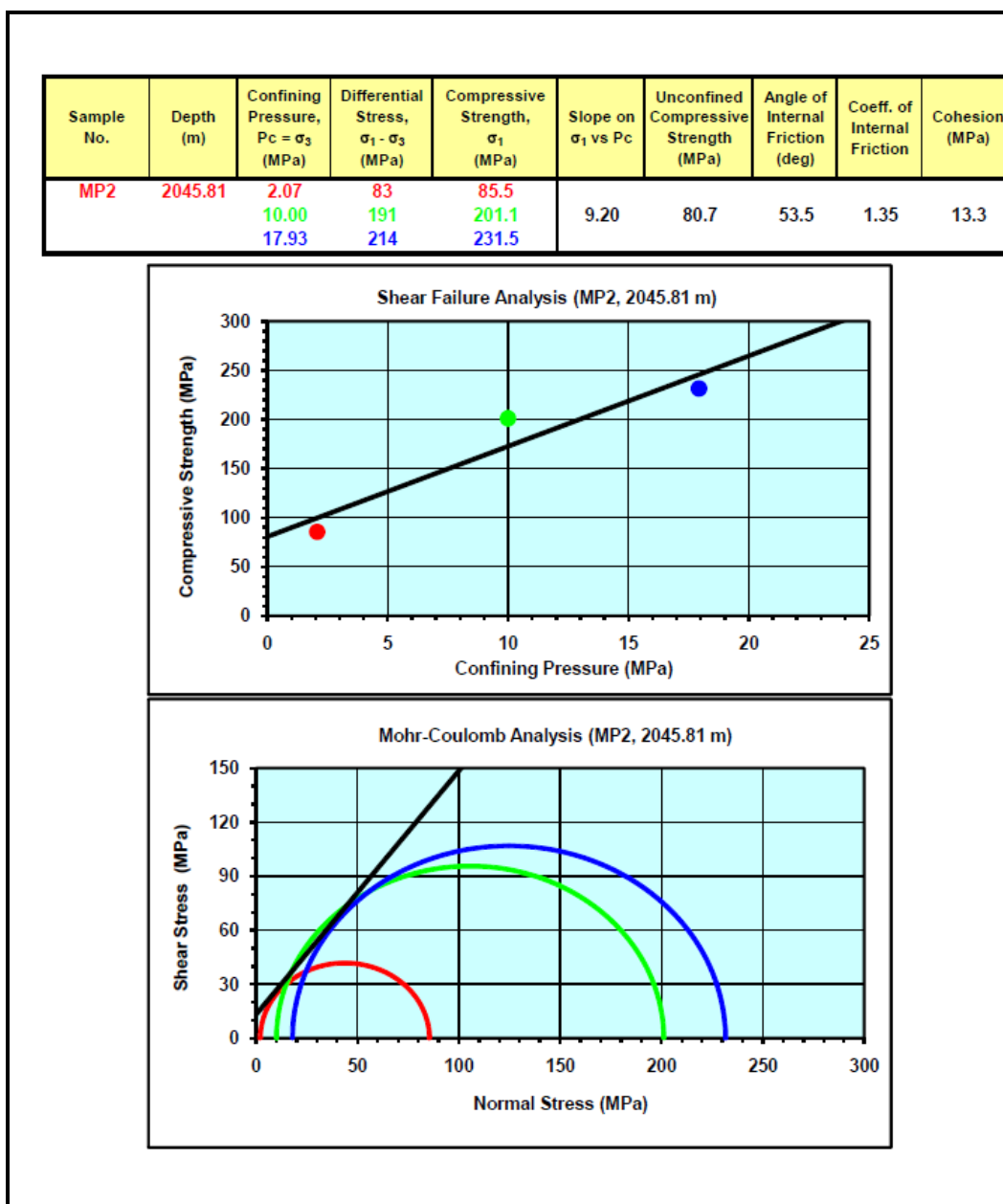


Figure 4-4: Mohr-Coulomb Failure Analysis Results

As shown in the preceding Figure, the angle of internal friction determined from the results of the multi-stage triaxial compressive strength test was 53.5 degrees with a cohesion value of 13.3 MPa (1,929 psi). The unconfined compressive strength determined from the Mohr-Coulomb failure analysis was 80.7 MPa (11,700 psi).

4.2 Cap Rock Integrity Testing

For a deep saline aquifer to be a successful candidate for acid gas sequestration, the overlying cap rock must be sufficiently thick and continuous to maintain a competent seal under acid gas injection conditions. The purpose of this phase of the core studies was to investigate the integrity of the overlying Ft. Simpson and Muskwa shales under the maximum injection pressure

and temperature operating conditions proposed by Spectra Energy so as to ensure that the injected gases will be confined to the Sulphur Point, the primary sequestration formation.

Appropriate shale samples were selected for testing based on CT analysis of the full diameter core material by selecting dense, non-fractured intervals. Full diameter samples from the top two formations, the Ft. Simpson and Muskwa shales, were cut from the core and subjected to cap rock testing protocol.

Sample: CR-1A Depth: 2031.0 m Formation: Ft. Simpson

Sample: CR-2A Depth: 2048.0 m Formation: Muskwa

Refer to **Figure 4-5** and **Figure 4-6** for CT photos of the two selected shale cored sections.

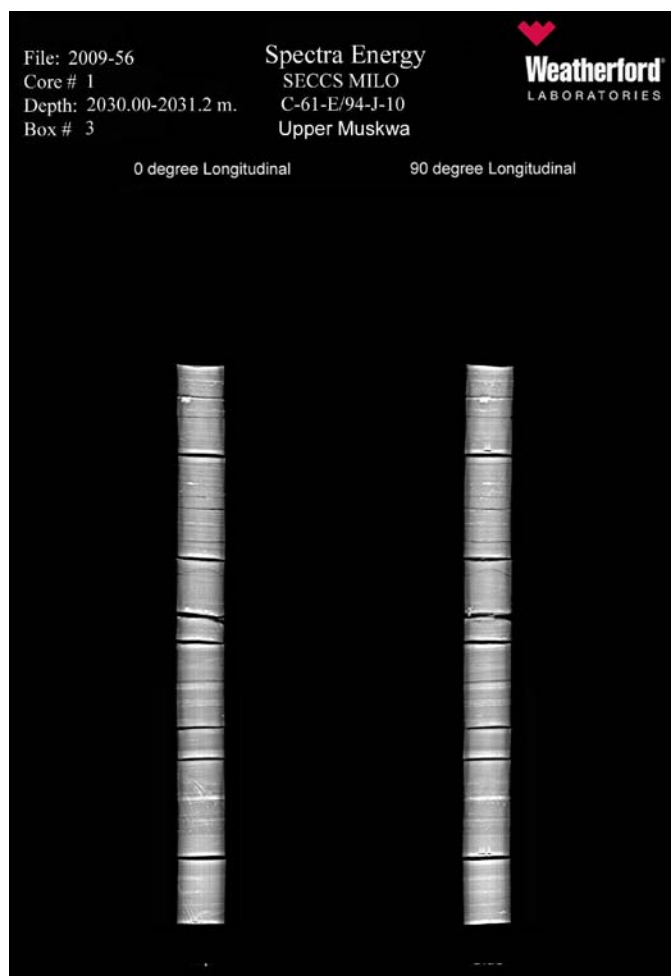


Figure 4-5: CT Scan for Ft. Simpson Shale Core Sample (2031.0 m)



Figure 4-6: CT Scan for Muskwa Shale Core Sample (2048.0 m)

Weatherford utilised a standard full diameter core flood displacement equipment to evaluate the cap rock integrity of both of the shale samples as per the following general test procedure:

1. Mount full diameter core sample in a ductile lead sleeve to allow vertical permeability measurements along the long axis of the full diameter core section (i.e. the same direction that the injected gases would traverse the cap rock).
2. Apply nominal overburden pressure and pore pressure.
3. Apply variable differential pressure with fresh water at 20°C.
4. Heat to 119°C, maintaining overburden and pore pressure (to ensure single phase water is maintained) and apply variable delta P to measure stable permeability to equilibrium brine at 119°C. It is expected that the initial permeability of the sample will be at or near zero unless fractures are present in the core.
5. While maintaining the pore pressure, switch the fluid over to brine saturated acid gas at appropriate pore pressure and overburden pressure at 119°C to simulate active contact of injected gas with the cap rock seal. Gradually increase the pressure levels up to an estimated peak injection pressure of 10,000 kPa (1,450 psi) to measure the effective acid gas permeability at reservoir conditions.

For successful cap rock evaluation, the effective permeability to formation water should be less than 0.001 mD. In addition, competent cap rock should be able to resist acid gas intrusion at a differential pressure of up to 7000 kPa (1,015 psi).

Table 4-2 and **Table 4-3** summarise the TIP data for the Ft. Simpson and Muskwa cap rock samples, respectively. **Table 4-4** provides a comparison to other cap rock quality data samples extracted from several other pertinent sources (References 7 and 8). The TIP results indicate very good cap rock competence in the presence of acid-gas both in the gas and fluid (brine) phases. The TIP is typically determined from the first pressure at which the acid gas can actually be forced into the rock matrix allowing a finite permeability to be measured.

For the Ft. Simpson and Muskwa shale samples, the TIP for acid-gas saturated brine was 5500 kPa (800 psi). The absolute effective permeabilities were 0.0000046 mD (4.6 nano Darcy) and 0.0000009 (0.9 nano Darcy), respectively, for the formation brine. Both of these values are many orders of magnitude less than 0.001 mD.

Table 4-2: Cap Rock Integrity Test Results for Ft. Simpson Shale

Milo Area, Lower Ft. Simpson/Transition Formation			
CORE & TEST PARAMETERS			
Well Location:	c-61-E/ 94-J-10	Length (cm):	8.08
Core I.D.:	CR-1A	Diameter (cm):	9.91
Porosity (fraction):	0.033	Pore Pressure (kPa):	20000
Air Permeability (mD):	0.03	Total Overburden (kPa):	41400
Test Temperature (°C):	119		
PERMEABILITY SUMMARY			
Test Phase		Permeability (mD)	
Permeability to: Formation Brine (Forward Direction)			
5500 kPa Total Injection Pressure		0.0000046	
10000 kPa Total Injection Pressure		0.0000071	
Permeability to: Acid Gas (Forward Direction)			
2070 kPa Total Injection Pressure		no flow	
3450 kPa Total Injection Pressure		no flow	
5500 kPa Total Injection Pressure		no flow	
7580 kPa Total Injection Pressure		no flow	
10000 kPa Total Injection Pressure		no flow	

Table 4-3: Cap Rock Integrity Test Results for Muskwa Shale

Milo Area, Muskwa Formation			
CORE & TEST PARAMETERS			
Well Location:	c-61-E/ 94-J-10	Length (cm):	10.2
Core I.D.:	CR-2A	Diameter (cm):	6.63
Porosity (fraction):	0.026	Pore Pressure (kPa):	20000
Air Permeability (mD):	1.1	Total Overburden (kPa):	41400
Test Temperature (°C):	119		
PERMEABILITY SUMMARY			
Test Phase		Permeability (mD)	
Permeability to: Formation Brine (Forward Direction)			
5500 kPa Total Injection Pressure		0.0000009	
10000 kPa Total Injection Pressure		0.0000031	
Permeability to: Acid Gas (Forward Direction)			
2070 kPa Total Injection Pressure		no flow	
3450 kPa Total Injection Pressure		no flow	
5500 kPa Total Injection Pressure		no flow	
7580 kPa Total Injection Pressure		no flow	
10000 kPa Total Injection Pressure		no flow	

Table 4-4: Summary of Shale Cap Rock Integrity Results

Fluid System	Lithology	Porosity (%)	Absolute Brine Permeability (nanoD)	Reservoir Pressure (kPa)	Reservoir Temperature (°C)	TIP (kPa)
Ft. Simpson - Acid Gas/Brine	Shale	3.3	4.6	20,000	119	5500
Muskwa - Acid Gas/Brine	Shale	2.6	0.9	20,000	119	5500
Colorado - CO ₂ /Brine	Shale	4.4	78.8	20,000	43	172
Calmar - CO ₂ /Brine	Shale	3.9	2.94	12,250	43	72,827

From **Table 4-4** it is evident that both the Colorado and Calmar shale sequences have initial absolute permeabilities to brine comparable to the Ft. Simpson and Muskwa shales of the Milo c-61-E well. Furthermore, since both the Ft. Simpson and Muskwa shales were found to be impermeable to acid gas at the maximum differential pressure applied in the laboratory (10,000 kPa or 1,450 psi), each of the two shale units in the Milo c-61-E wells is thus judged to be competent cap rock material. It can thus be concluded that unless either of these two cap rock intervals is very thin in vertical extent and exposed to extremely high overpressure in the acid gas injection zone, in contrast to the pressure on the upper side of the cap rock interval, any appreciable flow of acid gas over a non-geological time scale would be minimal to non-existent.

5.0 RELATIVE PERMEABILITY TESTING

Accurate modelling of the multiphase flow of supercritical acid gas in deep saline aquifers for acid gas sequestration (for both cycles of drainage during injection and imbibition during acid gas migration) is critical to understand the behaviour of the injected acid gas over extended time periods. Specifically, there is a need to determine the characteristics of the displacement processes involving the injected gas and in-situ fluids, the most important being the relative permeability and the residual gas saturation. Knowledge of both the shape and the end points of the relative permeability curves is essential to understand the efficiency of the displacement processes and the fate of the plume of injected acid gas.

As discussed previously in the Introduction, the original coring program was intended to capture core from both the various shale cap rock sequences as well as the highly porous and permeable sections of the Milo c-61-E well that had been previously identified as candidates for acid gas sequestration. Unfortunately, due to the very heterogeneous, vuggy character of the Sulphur Point and Slave Point target sequestration intervals, it was not possible to obtain representative cores from these two intervals for testing. Accordingly, only three full diameter core samples, two from the Lower Slave Point and one from the Lower Keg River section were recovered. The routine core measurements from these three cores are summarised in **Table 2-3**. From the air permeabilities shown in this table, it is obvious that all of the core samples used for the relative permeability testing were obtained from what should be considered as rock matrix and not the main reservoir rock, likely containing numerous fractures and vugs, that will ultimately comprise the target injection zone(s). Moreover, once it had been recognised, based on the routine core permeability measurements, that the Lower Keg River core sample represented non-reservoir rock, the relative permeability testing on the third sample, REL K-3, was cancelled.

It should be noted that the three samples used for the relative permeability testing were epoxyed prior to testing due to the presence of large vugs. Photos of the pre-test and post-test core samples are shown in Appendix D of Reference 4. Based on examination of these photos, the routine core analysis results of the post-test samples (specifically, the rock permeabilities) were considered to be more representative of the actual test samples and hence, have been used in the relative permeability test tables and figures reported in this section.

Synthesised formation brine was pressure saturated with synthesised acid gas at the reservoir pressure of 20.0 MPa (2,900 psi) and reservoir temperature of 119°C (246 °F) to obtain equilibrium live brine. The solubility of acid gas in the equilibrium brine was measured as 24.2 m³/m³. The viscosity of the equilibrium brine was measured by a capillary viscometer as 0.22 mPa.s (0.22 cP). The viscosity of acid gas was calculated as 0.034 mPa.s (0.034 cP) using WinProp simulation software (developed by Computer Modeling Group Ltd.).

The core samples to be tested were mounted using the equipment outlined in the "General Displacement Test Equipment" section of Reference 4. The core samples were maintained at the specified reservoir temperature of 119°C (246 °F) and a total overburden pressure of 41.4 MPa (6,000 psi) was applied to simulate the net effective pore pressure in the reservoir. The laboratory net overburden stress was corrected using Poisson's ratio to account for the tri-axial stress condition exerted on the sample in the core holder. This correction ensures that field stress load conditions are duplicated to yield representative rock compression and realistic absolute permeability values.

The following procedures were utilised for the acid gas/brine (primary drainage process) and brine/acid gas (secondary imbibitions process) relative permeability testing program:

1. The full diameter core samples were mounted in a lead sleeve and a hydrostatic core holder in the vertical direction so that flow will be parallel to the natural bedding planes.
2. The full diameter sample was evacuated to remove all trapped gas and then net reservoir overburden pressure was applied.
3. The sample was then pressure saturated with synthetic formation brine at reservoir pressure and temperature conditions. An initial absolute permeability to the formation brine was measured.
4. Acid gas saturated formation brine (live brine) was displaced through the core until a constant, stabilised GWR was recorded for the injection brine and the effluent brine. The absolute permeability to live brine was measured to establish the baseline permeability value for the relative permeability relationship.
5. An unsteady-state displacement with supercritical-phase acid gas was then conducted. The core was oriented vertically and this phase of the test was carried out in a base up fashion to simulate the flow direction that would occur in the reservoir with acid gas advancing from a sequestration zone below the cap rock. The injection of the acid gas was continued until flood out conditions were achieved. The total acid gas and brine flow rates as well as the pressure drop during the core flood were monitored. (The long term injection profile recorded in this phase of the study also indicates any potential for formation damage to the injection zone due to acid gas exposure).
6. The final irreducible water saturation, the maximum acid gas saturation, the endpoint permeability and the relative permeability to acid gas were measured.
7. A secondary imbibition test was then conducted by switching the injection fluid to acid gas-saturated brine (top down displacement). This phase of the test determines the level of “trapped” acid gas saturation when the aquifer advances into an area previously swept by acid gas contact and evaluates the long term mobility of the acid gas plume.
8. The sample was displaced with brine until the pressure drop across the core was stable and the produced water was only the water of condensation from the brine saturated acid gas (i.e. the acid gas saturation reaches the irreducible level). The end point water permeability to acid gas at this flood out condition was measured at multiple rates to ensure that the endpoint permeability data was representative and to examine the presence of any end effects induced by capillary pressure.
9. Using the fluid rates and the pressure drop history data, the acid gas and brine relative permeability curves were generated using Weatherford’s “history matching” numerical computer simulation program (refer to Appendix E of Reference 4).

An unsteady-state relative permeability test schematic is presented in **Figure 5-1**.

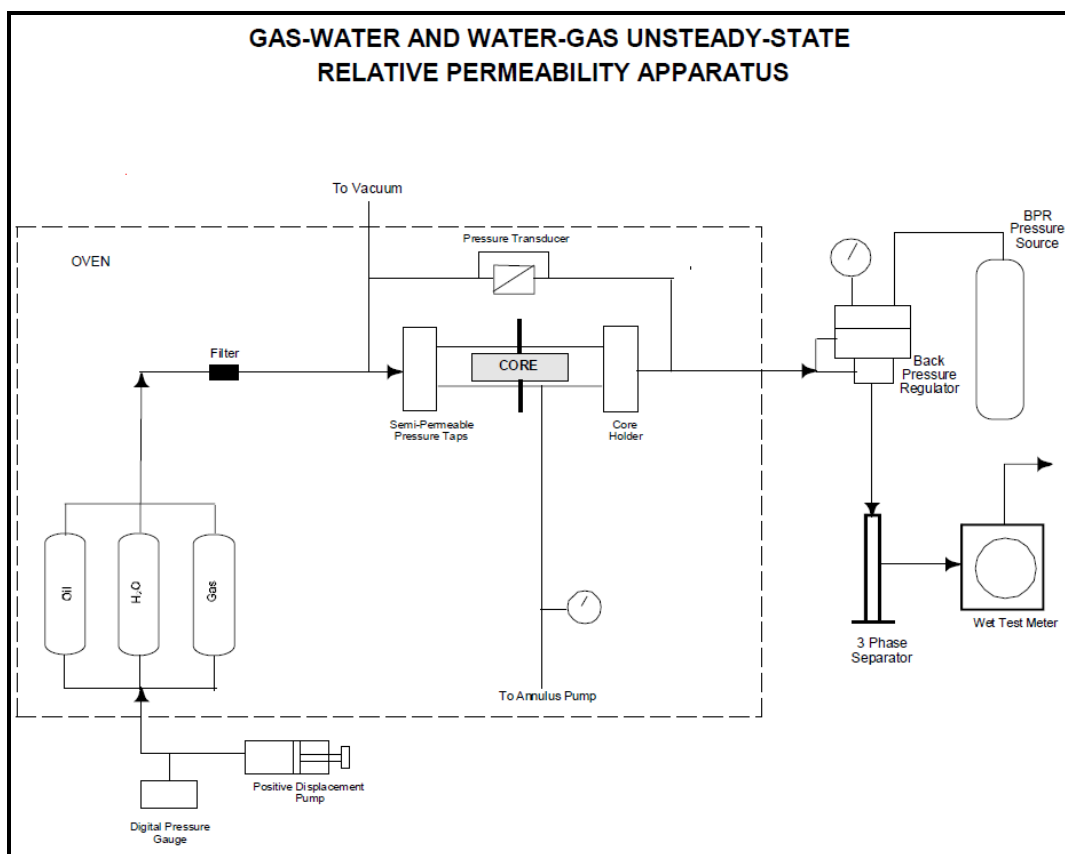


Figure 5-1: Unsteady State Relative Permeability Test Schematic

Table 5-1 and **Table 5-2** provide the drainage and imbibition acid gas/equilibrium brine relative permeability characteristics, respectively, of the two Lower Slave Point samples tested. Included in these tables are the Corey exponents for both the brine and the acid gas displacements as well as the sweep efficiencies of the acid gas and the brine during the primary drainage and secondary imbibition phases, respectively.

Table 5-1: Summary of Acid Gas/Equilibrium Brine Relative Permeability Results - Primary Drainage

Sample (or Rock Group)	Initial Absolute k_{brine} @ 100% Saturation (mD)	$k_{r \text{ CO}_2}$ @ Irreducible Brine Saturation	$S_{\text{brine-irr}}$	Corey Exponent for Brine	Corey Exponent for Acid Gas	Recovery Efficiency (fraction of brine)
REL K-1	0.0082	0.809	0.380	1.41	1.56	0.62
REL K-2	0.0065	0.875	0.308	1.85	1.34	0.69
Low k Carb.	2.05	0.435	0.487	1.80	4.18	0.51
Wab #1	0.018	0.529	0.595	1.4	5.6	0.41
Colorado shale	0.0000788	0.0148	0.605	6.5	2.6	0.40
Calmar shale	0.00000294	0.1875	0.638	1.3	2.5	0.36

Table 5-2: Summary of Acid Gas/Equilibrium Brine Relative Permeability Results - Secondary Imbibition

Sample (or Rock Group)	$k_{r \text{ brine @}}$ Irreducible Acid gas Saturation	$S_{\text{CO}_2\text{-irr}}$	Corey Exponent for Brine	Corey Exponent for Acid Gas	Recovery Efficiency (fraction of acid gas)
REL K-1	0.563	0.296	1.66	1.80	0.52
REL K-2	0.166	0.262	1.74	4.83	0.62
Low k Carb.	0.107	0.335	3.67	2.92	0.35
Wab #1	n/a	n/a	n/a	n/a	n/a
Colorado shale	0.0024	0.349	4.3	3.5	0.12
Calmar shale	0.282	0.256	4.0	2.2	0.29

As for the mercury injection capillary pressure data, the relative permeability characteristics of the three different permeability groupings of carbonate rocks (Reference 7) as well as two shale sequences for which laboratory data are available (Reference 8) are also summarised at the base of **Table 5-1** and **Table 5-2**.

Based on these definitions, the two Milo c-61-E Lower Slave Point core samples, with (post-test) permeabilities of 1.9 and 0.43 mD, respectively, would both represent “low permeability” carbonates. The Wabamun #1 sample relative permeability results, also taken from Reference 7, have once again been included in these two tables since this reservoir rock appears to be most comparable to the two c-61-E Lower Slave Point core samples.

Figure 5-2 and **Figure 5-3** illustrate the drainage and imbibition relative permeability curves for each of the two Lower Slave Point rock samples.

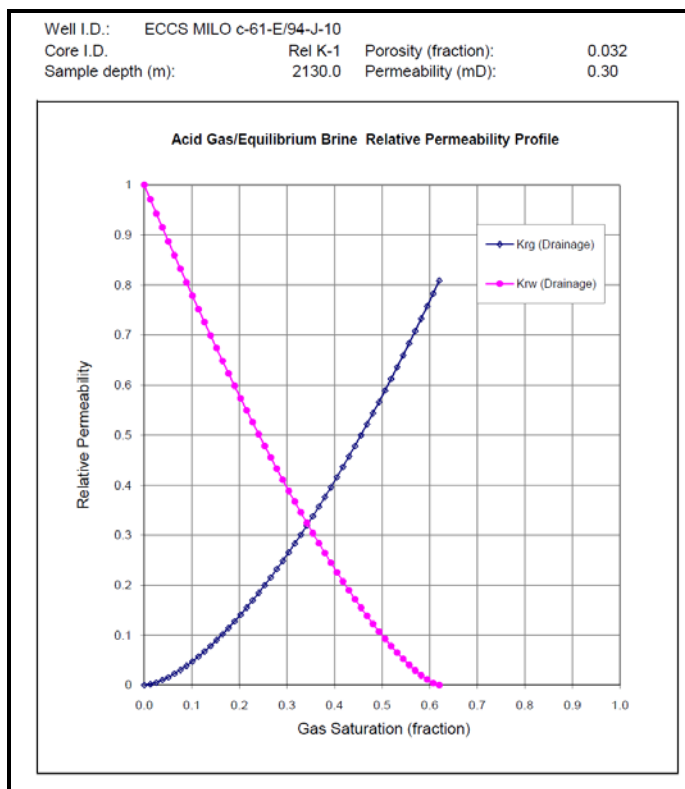


Figure 5-2: Acid Gas/Equilibrium Brine Relative Permeability Test Results - Primary Drainage

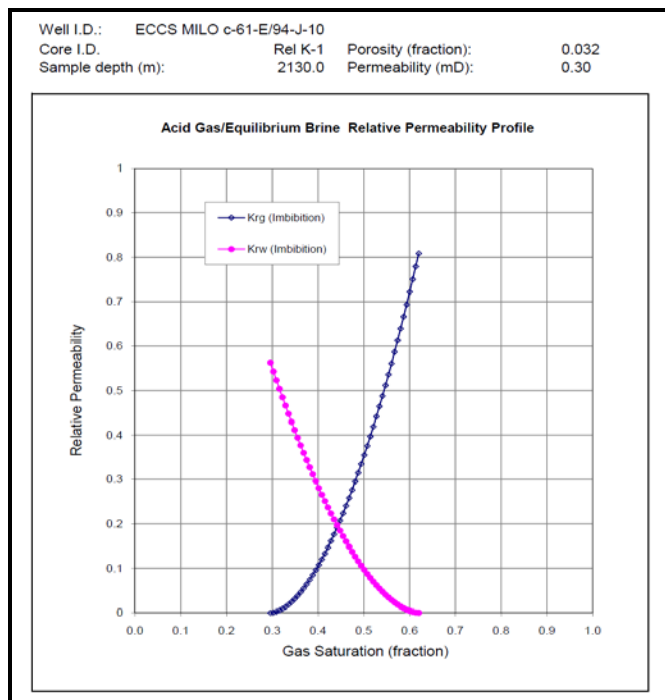


Figure 5-3: Acid Gas/Equilibrium Brine Relative Permeability Test Results - Secondary Imbibition

It is also instructive to compare the relative permeability curves for the two Milo c-61-E Lower Slave Point samples with those reported previously in References 7 and 8 for the composite

“low” permeability carbonate rocks and typical shale cap rocks, respectively. These results are graphed in **Figure 5-4** and **Figure 5-5**.

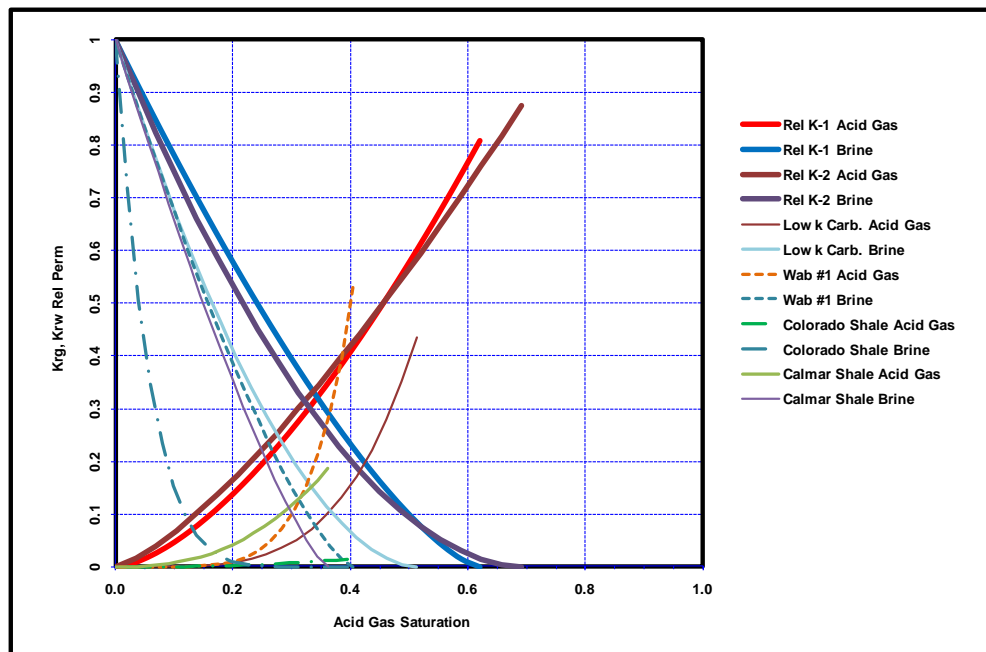


Figure 5-4: Comparison of Lower Slave Point Drainage Curves with “Low” k and Shale Zones

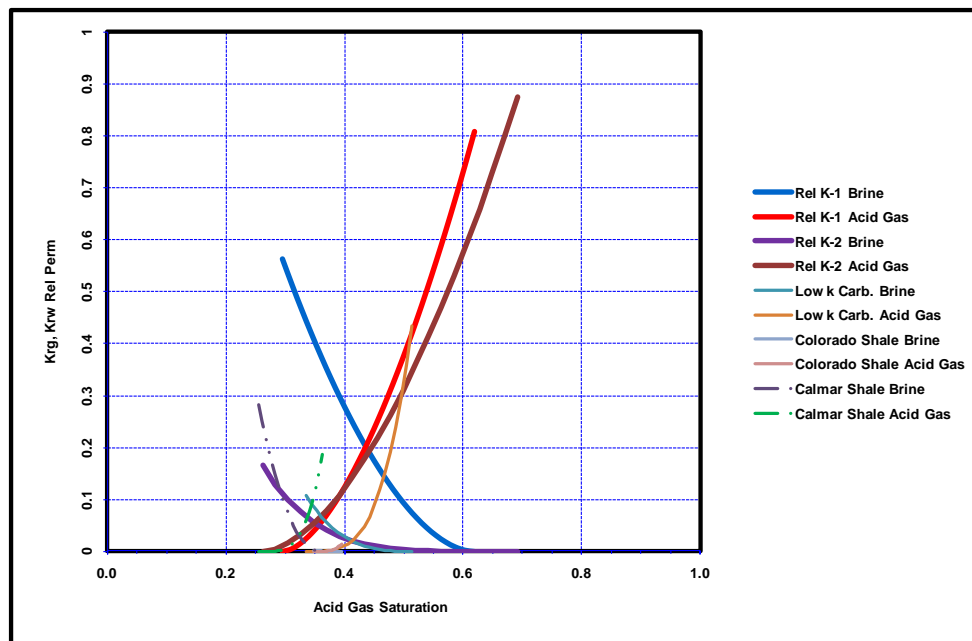


Figure 5-5: Comparison of Lower Slave Point Imbibition Curves with “Low” k and Shale Zones

Examination of the relative permeability data for the Lower Slave Point samples, in conjunction with both the published data for selected shale samples as well as the low permeability carbonate samples suggests that:

1. In contrast to typical “low” permeability carbonates, where the Corey exponents are significantly higher for the acid gas phase than for the brine phase during the drainage testing, the Corey parameters for each of the Lower Slave Point samples during the drainage cycle are relatively low and fairly close to one another with the Corey exponent for the brine phase for the REL K-2 sample actually being higher than that for the acid gas phase. These low Corey exponents imply less concave relative permeability curves, suggesting a reduction in multiphase interference effects compared to the composite set of low permeability carbonates discussed in Reference 7.
2. During the imbibition cycle, the Corey exponents for the REL K-1 sample remain low and are comparable to those for the drainage phase. In contrast, the Corey parameter for acid gas phase for the REL K-2 sample during imbibition is substantially higher and exceeds the acid gas Corey exponent for both the “low” permeability carbonate as well as both of the shale samples studied in Reference 8.
3. The similarity between and the low values for the Corey model parameters for each of the brine and acid gas phases for both the drainage and imbibition cycles of the two Lower Slave Point core samples (excepting the imbibition cycle for REL K-2) suggest that the processes of acid gas displacing brine and brine displacing acid gas are equally efficient and should not be subject to any significant degree of multiphase interference effects.
4. While the general rule of thumb for drainage and imbibition curves states that the Corey exponents are generally greater for a phase when its saturation is begin decreased than when it is being increased, the data summarised in **Table 5-1** and **Table 5-2** shows roughly an equal proportion of those Corey coefficients for brine that are higher for the drainage phase versus the imbibition cycle. The same observation is true for the Corey exponents describing the acid gas relative permeability behaviour during the imbibition phase.
5. The end point relative permeability to acid gas at the irreducible brine saturation for the primary drainage cycle averaged 0.84 of the initial absolute brine permeability for the two c-61-E Lower Slave Point core samples and is almost double the value observed (0.43) for the “low” permeability carbonate grouping evaluated in Reference 7 although this sample grouping has a significantly higher initial permeability to brine. This observation may be related to specific variations in the pore structure between the various samples that were tested. The higher end point permeability to acid gas for the two Lower Slave Point sections indicates a reasonably high sweep efficiency of brine by the acid gas in these two low permeability but possibly more homogeneous sample intervals. This result has an obvious advantage in an acid gas sequestration operation. As expected, given the very low permeabilities for the Colorado and Calmar shales, the end point permeability to acid gas for the two Lower Slave Point core samples is much greater than for either of these two shale samples.
6. The relative permeability to brine at the trapped acid gas saturation varies considerably between the two Lower Slave Point core samples and is roughly 3.4 times higher for the REL K-1 sample versus REL K-2. There also appears to be no correlation between the end point relative permeability to brine and the trapped residual acid gas saturation.
7. The irreducible brine saturation after flooding with acid gas for the two Lower Slave Point core samples averaged 0.34 and did not vary substantially between the two Milo c-61-E samples. This result indicates that approximately 0.66 of the pore space can be filled with acid gas. This irreducible brine saturation is lower than those measured from either the “low” permeability carbonate or Wabamun #1 samples. This observation does not seem to correlate with the higher absolute brine permeabilities measured for both the low perm carbonates and the Wabamun #1 samples and suggests that the more heterogeneous

nature of the higher permeability pore systems may be contributing to this phenomenon, possibly via channeling and bypassing of tighter portions of the pore system in preference to flow in the more permeable channels. Not unexpectedly, the irreducible brine saturations for the two Lower Slave Point samples were also substantially lower than for the very low permeability shale samples.

8. The trapped acid gas saturation value averaged 0.28 (with minimal variance) for the two REL K-1 and REL K-2 core samples and was only marginally lower than that reported in Reference 7 for the composite set of “low” permeability carbonate samples. The Lower Slave Point trapped acid gas saturation was also similar to those values documented in the Reference 8 for the Colorado and Calmar shale sequences.

6.0 CO₂ AND H₂S SOLUBILITY TESTING

This phase of the reservoir engineering study was designed to evaluate the solubility of the acid gas mixture in formation brine at reservoir temperature and pressure conditions. Two tests, Bulk Solubility test and Preferential Solubility, were conducted.

6.1 Bulk Solubility Testing

For this phase of the solubility testing, the solubility of the “whole” gas is measured. As described previously, synthesised formation brine was saturated with synthesised acid gas at the reservoir pressure of 20.0 MPa (2,900 psi) and reservoir temperature of 119°C (246 °F) to obtain equilibrium live brine. This bulk solubility test was conducted by charging the cylinder in the PVT apparatus with a specified volume of the synthetic brine and then increasing temperature and pressure to the reservoir conditions noted above. The acid gas mixture was then introduced into the cylinder from the top until the brine is saturated. The excess free gas was then removed at the reservoir condition and the remaining saturated brine was then flashed to ambient pressure and temperature.

The solubility of acid gas in the equilibrium brine was measured as 24.1 m³/m³.

6.2 Preferential Solubility Testing

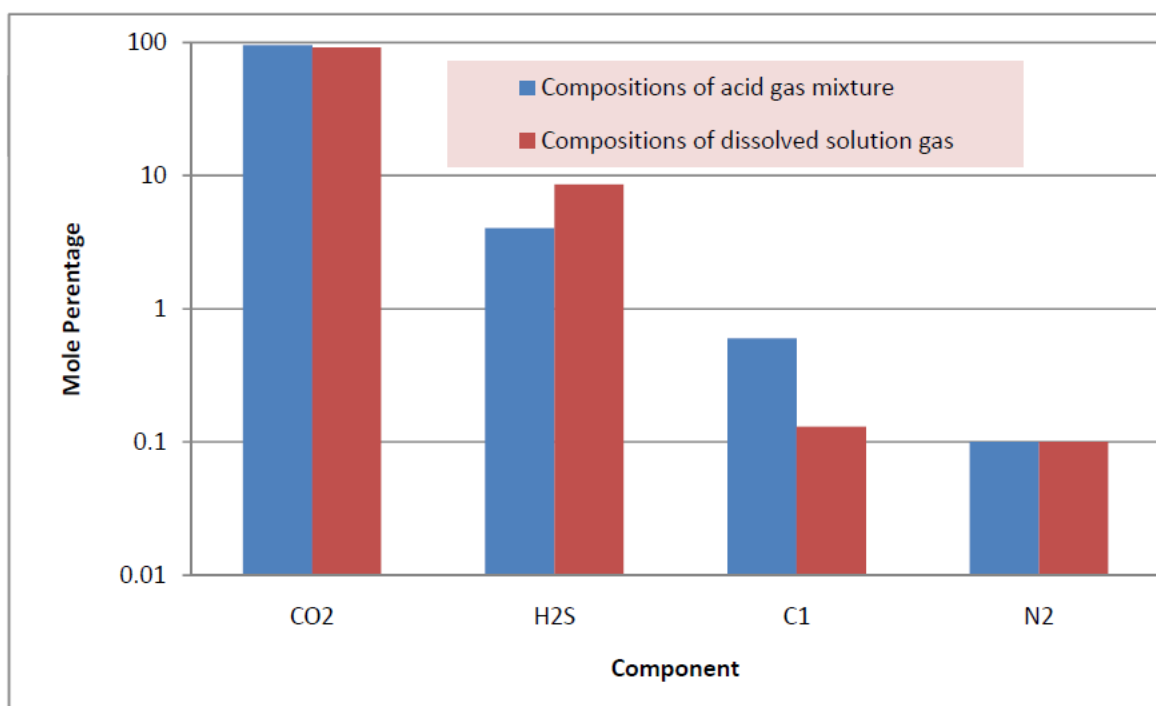
The preferential solubility test was conducted by charging the cylinder in the PVT apparatus with a specified volume of the synthetic brine and then increasing temperature and pressure to the same reservoir conditions noted above for the bulk solubility test. The acid gas mixture was then injected into the cylinder from the bottom by slowly bubbling through the brine phase at reservoir conditions until saturation occurred. The excess free gas was then removed at the reservoir conditions and the remaining saturated brine was flashed to ambient pressure and temperature.

Due to much the much higher affinity of H₂S than CO₂ for solubility in brine, H₂S gas will be selectively removed from solution to a much larger extent than CO₂ when a mixture of acid gas is exposed to the saturated brine. The compositions of the pre-test acid gas mixture as well as the gas dissolved in the brine were measured by GC (Gas Chromatography). The results are presented in **Table 6-1** on the following page.

Table 6-1: Results of Preferential Solubility Test

	Compositions of Acid Gas Mixture (mole percent)	Compositions of Dissolved Solution Gas (mole percent)
CO ₂	95.26	91.18
H ₂ S	4.04	8.59
C ₁	0.60	0.13
N ₂	0.10	0.10

Solubility of Acid Gas into Brine at Reservoir Conditions: 24.1 m³/m³



It should be noted that the prepared acid gas composition shown above is slightly different from the target acid gas mixture that was initially specified by Spectra (95% CO₂, 4.4% H₂S, 0.11% N₂ and 0.49% CH₄). The gas composition shown above is the actual one used for the relative permeability and the cap rock integrity testing and is considered to be within experimental accuracy of the anticipated plant gas composition provided Spectra.

The results shown in **Table 6-1** indicate that the H₂S component in the solution gas dissolved in the equilibrium brine increased from 4.04% to 8.59% in terms its mole fraction, while the CO₂ component decreased from 95.26% to 91.18% in terms its respective mole fraction.

7.0 REFERENCES

- ¹ Wellsite Geological Report - SECCS Milo c-61E/94-J-10, report by R.J. Patterson, P. Eng. for Spectra Energy CCS Services Inc., May 22, 2009.
- ² D.B. Bennion, F.B. Thomas, T. Ma and D. Imer, Hycal Energy Research Laboratories Ltd., "Detailed Protocol for the Screening and Selection of Gas Storage Reservoirs", SPE 59738, 2000.
- ³ D. Brant Bennion, F. Brent Thomas, Douglas W. Bennion, Ronald F. Bietz, Hycal Energy Research Laboratories Ltd., "Formation Screening to Minimize Permeability Impairment Associated With Acid Gas or Sour Gas Injection/Disposal", Petroleum Society of CIM and Canmet Paper NO. CIM 96-93
- ⁴ Reservoir Engineering Study: Ft. Simpson, Muskwa, Otter Park, Slave Point and Keg River Formations, Milo Area, report prepared for RPS Energy by Weatherford Laboratories, (Canada) Ltd., dated July 29, 2011
- ⁵ "Lease of a Storage Reservoir - Fort Nelson Carbon Capture and Storage Project", draft tenure document submitted to BC Titles by Spectra Energy, February 15, 2011.
- ⁶ "Petrographic Analyses of 10 Thin-Section Samples from Ft Simpson-Muskwa-Lower Slave Point-Lower Keg River Sections, Milo c-61-E/94-J-10", draft report submitted to Spectra Energy by Graham Davies Geological Consultants, July 2011.
- ⁷ D. Brant Bennion and Stefan Bachu, "Drainage and Imbibition CO₂/Brine Relative Permeability Curves at Reservoir Conditions for Carbonate Formations", SPE 134208, 2010.
- ⁸ D. Brant Bennion and Stefan Bachu, "Permeability and Relative Permeability Measurements at Reservoir Conditions for CO₂-Water Systems in Ultralow-Permeability Confining Cap Rocks", SPE 106995, 2007.

Appendix 1

Detailed Description of Coring Attempts at the SECCS Milo c-61-E/94-J-10 Well

DETAILED DESCRIPTION OF CORING OPERATIONS
(from SECCS Milo c-61-E/94-J-10 Wellsite Geological Report)

Cut Core #1 in Muskwa from 2027.6 - 2039.4 m MD and re-entered to attempt to core the Muskwa/Slave Point contact with Core #2 from 2039.4 - 2040.1 m. Jammed off on Core #2 and recovered only 0.35 m. Operator elected to case hole at that point due to apparent increased Ft Simpson shale sloughing.

Logged with Schlumberger (AIT-SP/CNL-LDT-GR-DAC) and ran 177.8 mm intermediate casing to 2040.25 m.

Drilled out of intermediate casing approximately half a metre and re-entered with core barrel to cut Core #3 from 2040.5 - 2058.6 m. Core jammed off on connection, resulting in recovery of approximately 9 m of Muskwa siltstone and approximately 0.3 m of dolomitic Slave Point rubble.

After cutting Core #3, drilled ahead to 2129 m in the Slave Point and attempted to cut Core #4 from 2129.0 - 2138.9 m. Cut 9.9 m and recovered 2.25 m of vuggy hydrothermal dolomite with typical chaotic bedding.

Attempted to cut Core #5 in the Slave Point from 2138.9 m but jammed off at 2143.2 m. Recovered 2.6 m of 4.3 m cut (all variably vuggy to dense hydrothermal dolomite).

After Core #5, re-entered and attempted to cut Core #6 from 2143.2 – 2144.6 m. Jammed off at 2144.6 m. Recovered 1.1 m of 1.6 m cut on Core #6 (hydrothermal chaotic bedded dolomite).

After Core #6, drilled ahead in interpreted dense hydrothermal dolomite fabric to anticipated possible porosity break indicated by ROP shift at 2157.1 m. Attempted to cut Core #7 from 2157.1 m but jammed off almost immediately at 2158.0 m. Recovered 0.8 of 0.9 m cut in Core #7, all of which showed similar hydrothermal dolomite fabric. Abandoned any further Slave Point coring attempts due to continual jamming, probably caused by large vugs adversely impacting the mechanical integrity of the rock.

After cutting Core #7, drilled ahead to 2213 m in interpreted Sulphur Point, at which point substantial lost circulation was encountered (up to 50% losses) No recognisably distinct Watt Mountain or Sulphur Point lithology was seen, although the Watt Mountain may have been represented by a slight decrease in crystal size in the monotonous dolomite sequence.

Drilled ahead partially blind with straight water through Sulphur Point and Keg River with extremely poor sample quality due to poor hole cleaning due to fluid loss and lack of adequate lifting capacity while water drilling.

At 2362.2 re-entered with core barrel to cut Core #8, in the Keg River. Cut 5.25 m from 2362.2 - 2367.35 m and recovered 2.5 m of hydrothermal dolomite after jamming off. Thereafter, drilled to 2387.0 m in the Keg River and cut Core #9 from 2387.0 - 2387.8 m. Jammed off again and recovered 0.5 m of dark dense dolomite out of 0.8 metre cut. Thereafter, drilled to FTD in tight, silica cemented Chinchaga sandstone. The Upper Chinchaga was characterised by calcareous lithographic aspect dolomite with increasing sandstone laminae below.

Appendix 2

Photos of Sampling Attempts in the Shale Zones

PHOTOS OF SAMPLING ATTEMPTS IN THE SHALE ZONES



PHOTOS OF SAMPLING ATTEMPTS IN THE SHALE ZONES



Appendix 3

Labeled Photos of All Core Samples Selected for Testing

Spectra Energy
SECCS MILO c-61-E/94-J-10
Core 1 Box 3
Upper Muskwa

Top: 2030.00 m



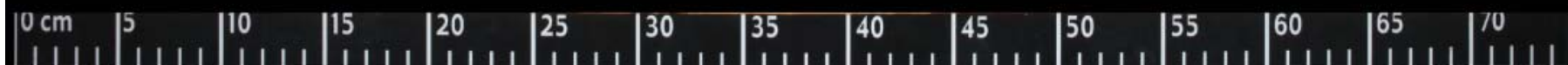
Bottom: 2031.20 m




Weatherford
LABORATORIES

Spectra Energy
SECCS MILO c-61-E/94-J-10
Core 3 Box 2
Lower Muskwa/Top Slave Point

Top: 2042.00 m



Bottom: 2043.40 m




Weatherford
LABORATORIES

Spectra Energy
SECCS MILO c-61-E/94-J-10
Core 3 Box 4
Lower Muskwa/Top Slave Point

Top: 2044.90 m

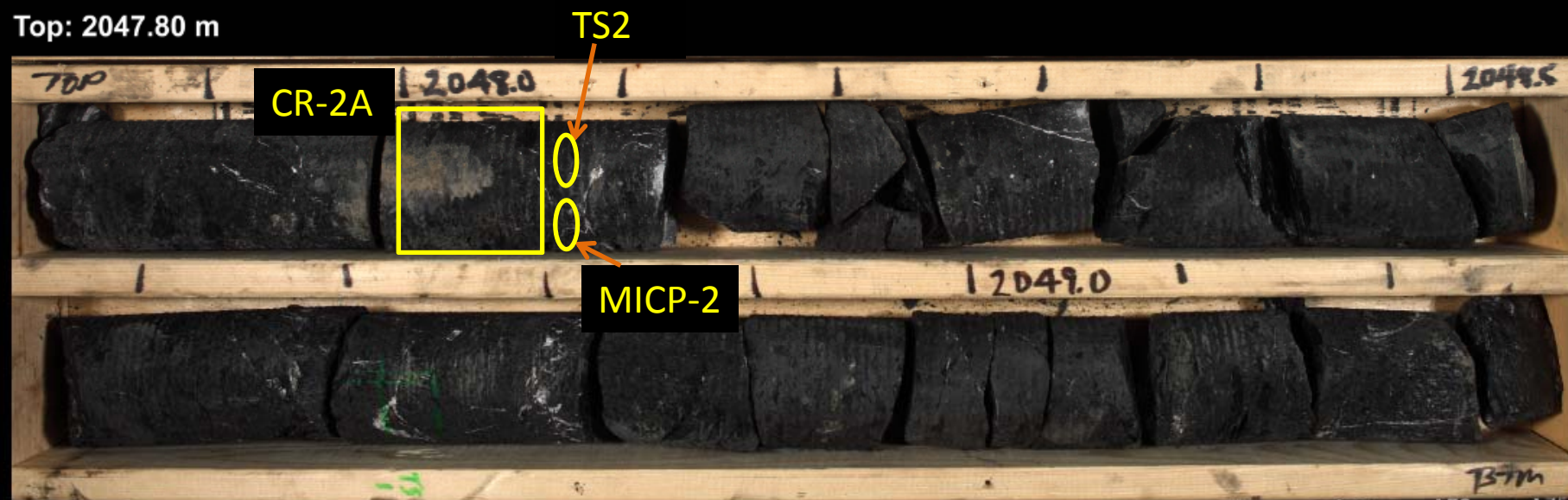


Bottom: 2046.35 m



Spectra Energy
SECCS MILO c-61-E/94-J-10
Core 3 Box 6
Lower Muskwa/Top Slave Point

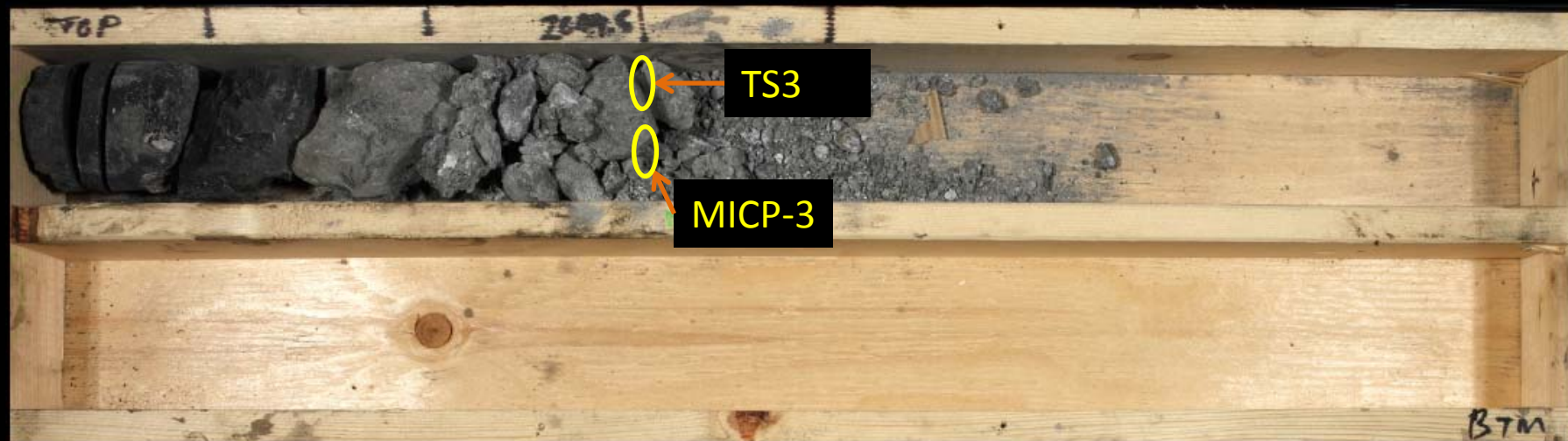
Top: 2047.80 m



Bottom: 2049.30 m

Spectra Energy
SECCS MILO c-61-E/94-J-10
Core 3 Box 7
Lower Muskwa/Top Slave Point

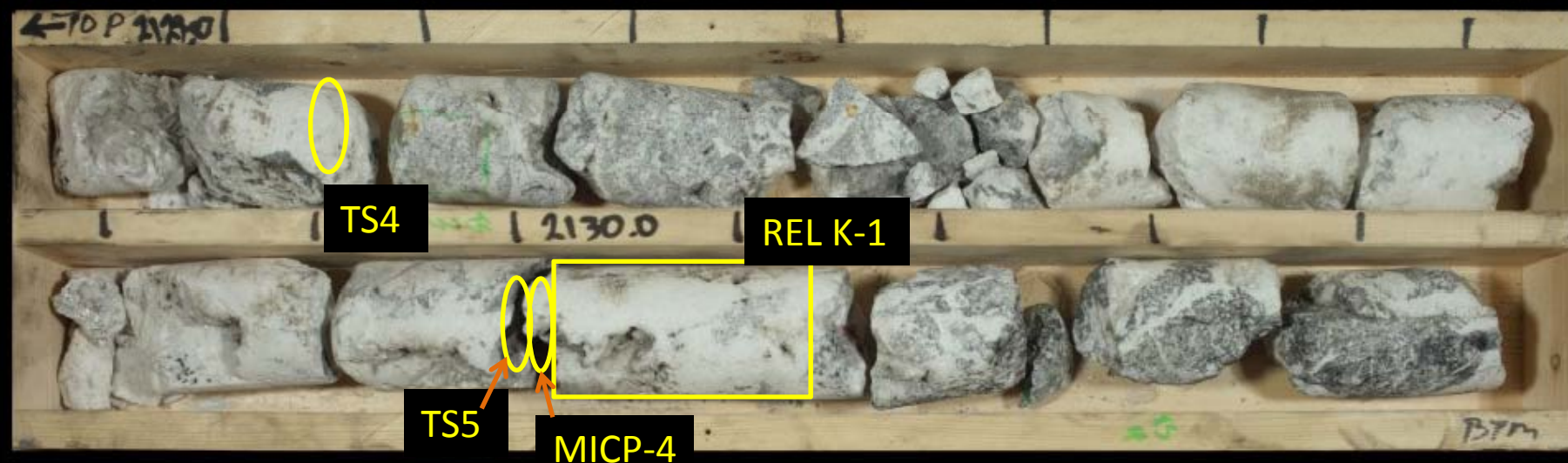
Top: 2049.30 m



Bottom: 2058.60 m

Spectra Energy
SECCS MILO c-61-E/94-J-10
Core 4 Box 1
Middle Slave Point

Top: 2129.00 m



Bottom: 2130.50 m




Weatherford
LABORATORIES

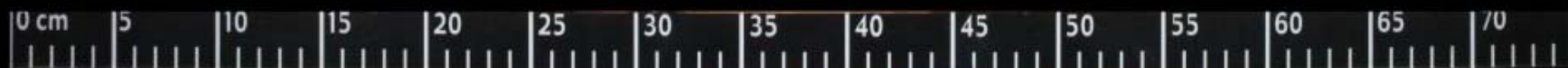
Spectra Energy
SECCS MILO c-61-E/94-J-10
Core 5 Box 1
Middle Slave Point

Top: 2138.80 m



Spectra Energy
SECCS MILO c-61-E/94-J-10
Core 5 Box 2
Middle Slave Point

Top: 2140.30 m



Bottom: 2141.00 m


Weatherford
LABORATORIES

Spectra Energy
SECCS MILO c-61-E/94-J-10
Core 6 Box 1
Middle Slave Point

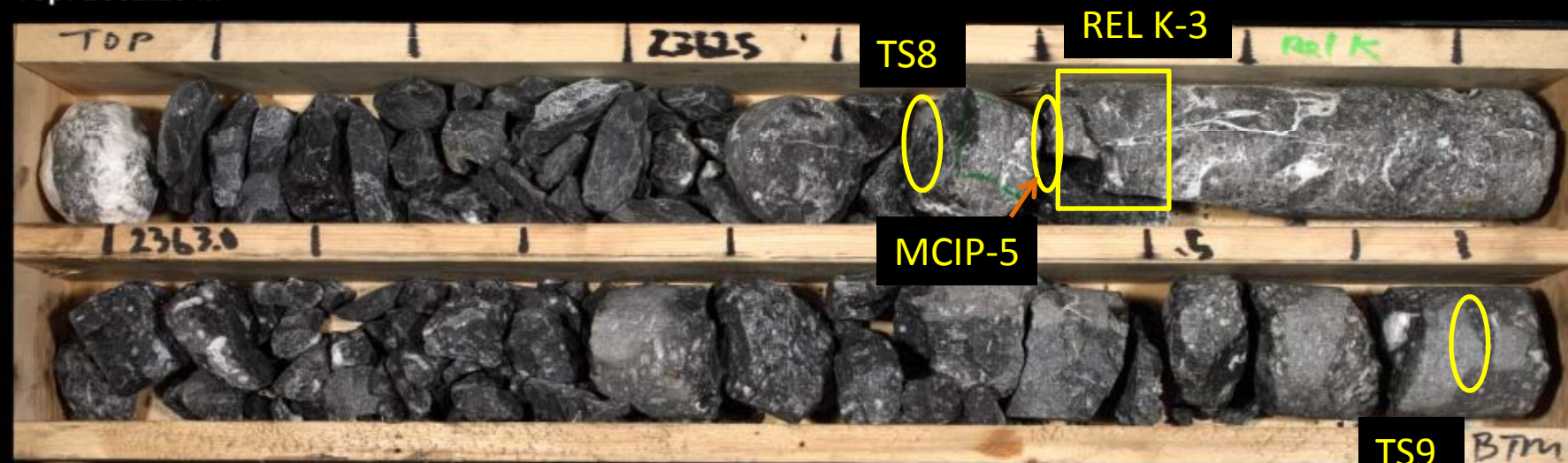
Top: 2143.20 m



Bottom: 2144.20 m

Spectra Energy
SECCS MILO c-61-E/94-J-10
Core 8 Box 1
Keg River

Top: 2362.20 m



Spectra Energy
SECCS MILO c-61-E/94-J-10
Core 9 Box 1
Keg River

Top: 2387.00 m



Bottom: 2387.80 m



Appendix 4

Understanding the Elastic Parameters

Understanding the Elastic Parameters

Introduction

The Rock Mechanics test is used to measure the elastic properties of the Muskwa cap rock material and confirm that this shale has a very high mechanical strength and will not experience significant changes in proportion (deformation) when high stresses are applied as evidenced by the minimal change in all the integrity indicators (compressive strength & elastic parameters) investigated by the test.

The results of these tests indicate that the strength of the Muskwa cap rock is much higher than the anticipated maximum operating pressure conditions of the Fort Nelson Milo acid gas sequestration project and consequently, establish the continued maintenance of cap rock integrity in the presence of injected acid gas fluids and pressures.

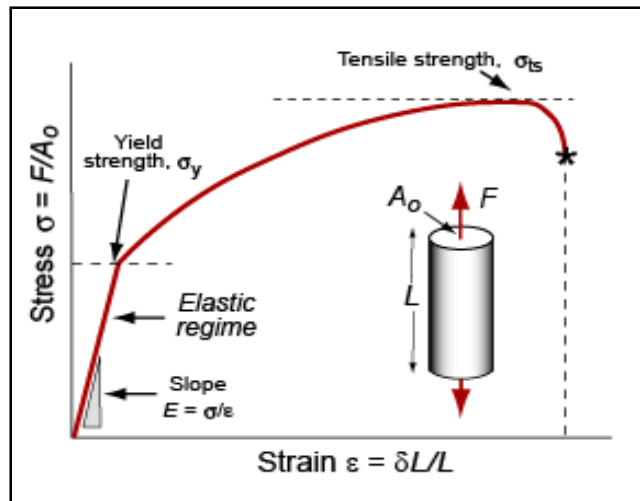
The tests to establish mechanical properties included;

- The compressive strength test which provided information on the cap rock strength and static elastic properties (static Young's Modulus & Poisson's Ratio).
- The ultrasonic test which provided both the compressional and shear wave velocities used to calculate the dynamic elastic properties (Dynamic Young's modulus, Bulk Modulus, Shear Modulus & Poisson's Ratio).

Definitions of the Elastic Parameters

The deformation of a sample in tension or compression is most conveniently expressed in terms of strain. Strain is the change in length per unit of length observed while applying force to the sample. Stress is more significant than force as it depends primarily on the cross section of the sample.

Appendix Figure 1 shows a typical tensile stress-strain curve generated through an unconfined tensile failure test. The initial portion of equally increasing stress and strain, up to the yield strength σ_y or elastic limit or proportional limit of the material, is linear (Hooke's law). While within this portion of the curve, the material is elastic, meaning that the strain is recoverable i.e the material returns to its original shape when the stress is removed. Stresses above the elastic limit cause permanent deformation or fracture depending on whether the material is brittle or ductile.

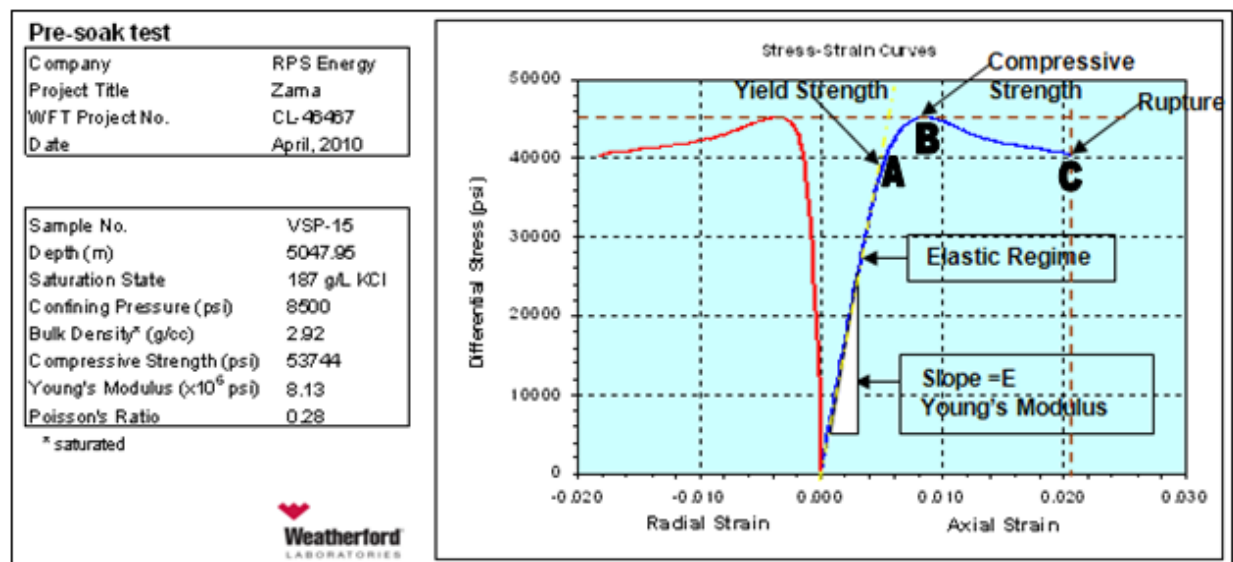


Appendix Figure 1: Typical Tensile Stress-Strain Curve

Source: Granta CES Edupack

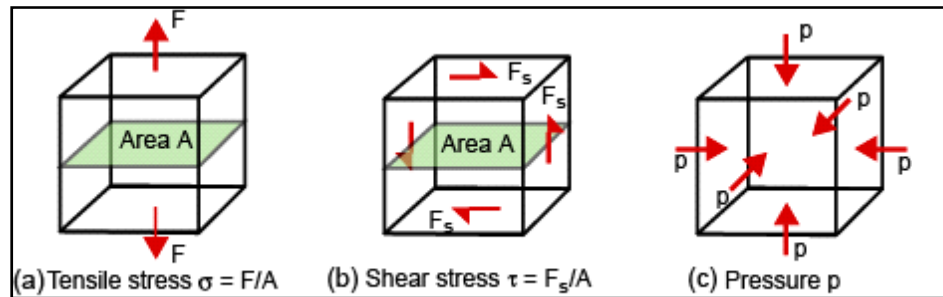
The stress strain curves generated for the subject shale samples were subjected to confined compression tests in order to generate the radial and axial stress-strain curves. Nevertheless, the resulting determination of rock strength parameters is similar.

After the yield point, the material experiences a permanent residual strain that is not lost on unloading called inelastic deformation as there's no force to drive the molecular structure back to its original position. As deformation continues, the stress increases until it reaches the ultimate (compressive) strength at point B. Between point A and point B some local deformation of the rock is occurring. Between point B and point C, additional failure occurs which typically results in small local fractures connecting up along a major sloping fracture plane through the sample.



Appendix Figure 2: Annotated Test Sample Report

Within the linear elastic regime, strain is proportional to stress, but stress can be applied in more than one way, Appendix Figure 2.



Appendix Figure 3: Stress Application

Source: Granta CES Edupack

The tensile stress, σ , produces a proportional tensile strain, ε :

$$\sigma = E \varepsilon$$

and the same is true in compression. The constant of proportionality, E , is called **Young's Modulus**.

Young's Modulus (or Modulus of Elasticity) E , is the ratio of the applied stress to the fractional extension (or shortening) of the sample length parallel to the tension (or compression). The strain is the linear change in dimension divided by the original length.

Relationship between Young's Modulus and the other elastic constants, Poisson's ratio, Shear & Bulk moduli;

$$E = 2G(1+\nu) = 3K(1 - 2\nu)$$

where : E = Modulus of Elasticity; K = Bulk Modulus; G = Shear Modulus; ν = Poisson's Ratio

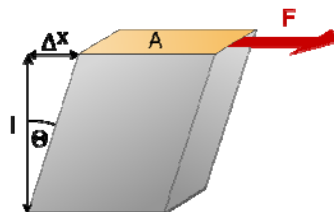
Similarly, a shear stress, σ_s causes a proportional shear strain, γ

$$\sigma_s = G \gamma$$

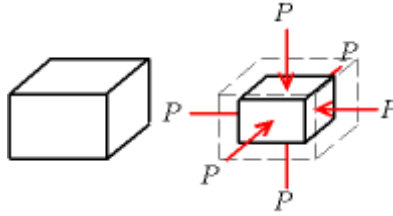
and a pressure p results in a proportional fractional volume change (or "dilatation") Δ :

$$p = K \Delta$$

where G is the shear modulus and K the bulk modulus.



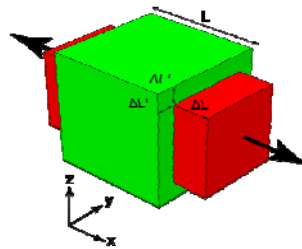
Shear modulus (or **modulus of rigidity**) is the ratio of the applied stress to the distortion (rotation) of a plane originally perpendicular to the applied shear stress.



Bulk Modulus of Elasticity is the ratio of stress to change in volume of a material subjected to axial loading.

All three of these moduli have the same dimensions as stress, that of force per unit area (N/m², Pa or psi).

Poisson's ratio is the ratio of the relative contraction strain, or transverse strain normal to the applied load, to the relative extension strain, or axial strain in the direction of the applied load.



Poisson's Ratio can be expressed as

$$\nu = - \epsilon_t / \epsilon_l$$

where

ν = Poisson's ratio; ϵ_t = transverse strain; ϵ_l = longitudinal or axial strain

Strain can be expressed as

$$\epsilon = dl/L$$

where

dl = change in length; L = initial length

The Poisson's ratio of a stable, isotropic, linear elastic material cannot be less than -1.0 nor greater than 0.5 due to the requirement that the elastic modulus, the shear modulus and bulk modulus have positive values. Most materials have Poisson's ratio values ranging between 0.0 and 0.5 . A perfectly incompressible material deformed elastically at small strains would have a Poisson's ratio of exactly 0.5 .

Dynamic elastic constants are determined by measuring elastic wave velocities in the material.

The velocity of a shear wave, (v_s) is controlled by the shear modulus,

$$v_s = \sqrt{\frac{G}{\rho}}$$

where

G is the shear modulus; ρ is the solid's density.

The bulk modulus K and the density ρ determine the speed of sound c (pressure waves), according to the Newton-Laplace formula

$$c = \sqrt{\frac{K}{\rho}}$$

The speed at which a wave travels through a medium may be expressed in two ways. Geophysicists think in terms of velocity, i.e., distance traveled per unit of time. Subsurface formation velocities range from 6000 to 25,000 ft/second. Log analysts think in terms of time, i.e., the time taken to travel one unit of distance. A convenient unit of measurement is the microsecond per foot (μ sec/ft) given the symbol Δt to signify *change in time*.

With these definitions in mind, the dynamic elastic constants of a medium can be expressed as a function of bulk density (ρ_b) and travel time for compressional and shear waves, Δt_c and Δt_s , respectively, as shown in the following table.

μ Poisson's Ratio	Lateral strain Longitudinal strain	$\frac{1/2 (\Delta t_s / \Delta t_c)^2 - 1}{(\Delta t_s / \Delta t_c)^2 - 1}$
G Shear Modulus	Applied stress Shear strain	$\frac{\rho_b}{\Delta t_s^2} \times a$
E Young's Modulus	Applied stress Normal strain	$2G (1 + \mu) \times a$
K_B Bulk Modulus	Applied stress Volumetric strain	$\rho_b \left(\frac{1}{\Delta t_c^2} - \frac{4}{3 \Delta t_s^2} \right) \times a$

Dynamically measured moduli are more accurate than the static moduli which are affected by contributions to strain from test equipment deflection or other material properties.